12. Johne R, Dremsek P, Kindler E, Schielke A, Plenge-Bonig A, Gregersen H, et al. Rat hepatitis E virus: geographical clustering within Germany and serological detection in wild Norway rats (*Rattus norvegicus*). Infect Genet Evol. 2012;12:947–56. http://dx.doi.org/10.1016/j.meegid.2012.02.021
13. Purcell RH, Engle RE, Rood MP, Kabrane-Lazizi Y, Nguyen HT, Govindarajan S, et al. Hepatitis E virus in rats, Los Angeles, California, USA. Emerg Infect Dis. 2011;17:2216–22. http://dx.doi.org/10.3201/eid1712.110482
14. Li TC, Yoshimatsu K, Yasuda SP, Arikawa J, Koma T, Kataoka M, et al. Characterization of self-assembled virus-like particles of rat hepatitis E virus generated by recombinant baculoviruses. J Gen Virol. 2011;92:2830–7. http://dx.doi.org/10.1099/vir.0.034835-0
15. Li TC, Suzaki Y, Ami Y, Dhole TN, Miyamura T, Takeda N. Protection of cynomolgus monkeys against HEV infection by oral administration of recombinant hepatitis E virus–like particles. Vaccine. 2004;22:370–7. http://dx.doi.org/10.1016/j.vaccine.2003.08.004

Address for correspondence: Tian-Cheng Li, Department of Virology II, National Institute of Infectious Diseases, 4-7-1 Gakuen, Musashi-murayama, Tokyo 208-0011, Japan; email: litc@nih.go.jp

Vaccine 31 (2013) 417–424

Contents lists available at SciVerse ScienceDirect

Vaccine

journal homepage: www.elsevier.com/locate/vaccine

Chimeric hepatitis E virus-like particle as a carrier for oral-delivery

Pitchanee Jariyapong[a,b,1], Li Xing[a,1], Nienke E. van Houten[c], Tian-Cheng Li[d], Wattana Weerachatyanukul[a,b], Benjamin Hsieh[a], Carlos G. Moscoso[a], Chun-Chieh Chen[a], Masahiro Niikura[c], R. Holland Cheng[a,*]

[a] Department of Molecular and Cellular Biology, University of California, 1 Shields Ave., Davis, CA 95616, United States
[b] Department of Anatomy, Faculty of Science, Mahidol University; Bangkok 10400, Thailand
[c] Faculty of Health Sciences, Simon Fraser University, Burnaby, B.C. V5A 1S6, Canada
[d] Department of Virology II, National Institute of Infectious Diseases, Tokyo 208-0011, Japan

ARTICLE INFO

Article history:
Received 14 July 2012
Received in revised form 12 October 2012
Accepted 19 October 2012
Available online 26 October 2012

Keywords:
Hepatitis E virus
Virus like particle
Recombinant capsid protein
HIV-1 epitope
Trypsin proteolysis
Quaternary structure

ABSTRACT

Oral delivery with virus-like particles (VLPs) is advantageous because of the inherited entry pathway from their parental viral capsids, which enables VLP to withstand the harsh and enzymatic environment associated with human digestive tract. However, the repeat use of this system is challenged by the self-immunity. In order to overcome this problem, we engineered the recombinant capsid protein of hepatitis E virus by inserting p18 peptide, derived from the V3 loop of HIV-1 gp120, into the antibody-binding site. The chimeric VLP resembled the tertiary and quaternary structures of the wild type VLP and specifically reacted with an HIV-1 antibody against V3 loop. Different from the wild type VLP, the chimeric VLP was vulnerable to trypsin cleavage although it appeared as intact particle, suggesting that the intermolecular forces of attraction between the recombinant capsid proteins are strong enough to maintain the VLP icosahedral arrangement. Importantly, this VLP containing the V3 loop did not react with anti-HEV antibodies, in correspondence to the mutation at its antibody-binding site. Therefore, the insertion of peptides at the surface antigenic site could allow VLPs to escape pre-existing anti-HEV humoral immunity.

1. Introduction

Development of an effective oral delivery system for mucosal vaccination would provide a convenient means for treatment or prevention of various human diseases because it could constrain the establishment and dissemination of infection at their primary entry site, thus provide the best window of opportunity in prevention of human diseases. Despite its high efficiency, there are only a limited number of oral vaccines currently available for human utilization, far less than the number of severe health problems caused by mucosal pathogens [1]. There are several difficulties in oral immunization with non-replicating molecules, such as low pH in the stomach, the presence of proteolytic enzymes in the digestive tract, and the presence of physical as well as biochemical barriers associated with the mucosal surface itself [2]. Non-replicating virus like particles (VLPs), that inherit cell entry pathway from the viral capsid, pose a great advantage in providing desired specificity on tissue targeting and gene protection [3,4] but the major hurdle comes from their self-immunity, as shown with polyomavirus-like particle [5].

Hepatitis E virus (HEV) is a non-enveloped ssRNA virus [6] that causes human acute hepatitis through primarily fecal-and-oral transmission [7]. HEV-VLPs is a T = 1 icosahedral virus-like particles with a diameter of 270 Å [8,9]. It is self-assembled from the truncated capsid protein when it is expressed in insect cells [10] and able to induce antigen-specific mucosal immunity after oral administration [11–13]. The structure of HEV-VLP reveals a unique structural modularity, i.e. the three domains of the truncated protein carry independently the biological functions [14–16]. While the N-terminal S domain (shell; amino acids 118–317) forms icosahedral base [14–16] and the adjacent M domain (middle; amino acids 318–451) builds up the three-fold plateau, the P (protruding; amino acids 452–606) domains exhibits profound HEV antigenicity [14,17,18], dimerization [19,20], and host recognition [21]. As a result, sequence modification at the P-domain will not interfere with HEV-VLP assembly as well as the stability of the VLP in acidic and proteolytic environment. In fact, a chimeric VLP carrying a peptide insertion at C-terminal end of the truncated capsid protein retains the T = 1 icosahedral organization [12]. If an insertion can be placed at antibody-binding site at the P-domain, the chimeric VLP may be able to escape from antibody-binding. However, it requires insertion of foreign epitope in the middle region of PORF2, and four

* Corresponding author. Tel.: +1 530 752 5659.
E-mail address: rhch@ucdavis.edu (R.H. Cheng).
[1] These authors have contributed equally to this work.

0264-410X/$ – see front matter © 2012 Elsevier Ltd. All rights reserved.
http://dx.doi.org/10.1016/j.vaccine.2012.10.073

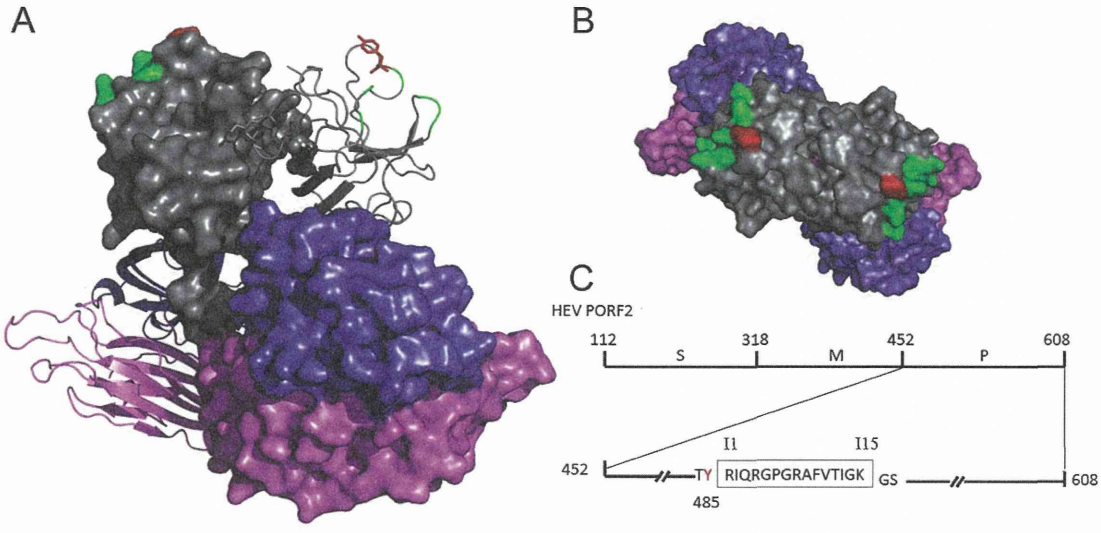

Fig. 1. Schematic diagram of the chimeric p18-VLPs. (A) side view of a PORF2 dimer colored in magenta for the S-domain, slate for the M-domain and gray for the P-domain. The residue Y485 (red stick) is overlapped with the binding site of HEP224 antibody (green colored surface). (B) Top view of the dimer showing the spatial arrangement of Y485 (red) and the binding site of HEP224 antibody (green). (C) Insertion of 15 amino acid residues of p18 (boxed; I1-I15) at the position 485 (red) of P-domain indicated by arrowhead (bottom). (For interpretation of the references to color in this figure legend, the reader is referred to the web version of the article.)

previous trials at residues A179, R366, A507 and R542 had all failed [12] because the insertions were found to inhibit the quaternary assembly of the VLP [22]. With the known crystal structure and a well-defined antibody-binding site, we selected an insertion site after residue Tyr485. Our results indicate that the chimeric VLP carrying the insertion at Tyr485 is stable within hydrolytic and proteolytic environments, and is thus suitable for oral delivery.

2. Results

2.1. Reaction of p18-VLP to antibodies

The P-domain of HEV organizes into a β-barrel consisting of two β-sheets, the F″A″Bb″ sheet and the Ba″E″D″C″ sheet. The residue Y485 is located at the A″Ba″ loop and is within the binding interface of HEP224, a conformational anti-ORF2 antibody. The A″Ba″ loop is positioned at the shoulder of the protruding P-domain and hangs down to cover a surface groove region. This leads to a slightly higher B-factor for the residues around Y485 and the groove provides sufficient space to accommodate additional amino acids (Fig. 1A and B). Thus the residue Y485 was identified as a promising candidate for insertion of a short peptide without interfering with either tertiary structure folding or capsid assembly.

To test our hypothesis, we constructed a fusion protein by inserting a 15-amino acid antigenic peptide, "p18", after residue Y485 on the P-domain of HEV-VLPs (Fig. 1C). The p18 epitope (RIQRGPGRAFVTIGK) is from the V3 loop of the HIV-1 Env subunit gp120, which is able to stimulate an HIV-1-specific cytotoxic T-lymphocyte (CTL) response [23]. The fusion protein was recovered after CsCl density gradient purification in a form of chimeric virus-like particles (Fig. 2A), referred as "p18-VLPs". We then assessed the reactivity of p18-VLP to two antibodies 447-52D and HEP224 specific against the V3 loop of HIV-1 Env gp120 and a conformational epitope of the wild type HEV, respectively. As a reference, the reactivity of 0.1 mg/ml wild-type HEV-VLP to antibody HEP224 was set as 100% (Fig. 2B). The antibody 447-52D was found to react preferably with the p18-VLPs (50% to 0.001 mg/ml and 100% to 0.1 mg/ml p18-VLP). Although nonspecific binding was observed in wild-type HEV-VLP at all concentrations, the level was constantly less than 30% reactivity. Strikingly, the reactivity of HEP224 to p18-VLPs was very low. Only 1–2% HEP224 reactivity to 0.1 mg/ml p18-VLP was detected, in contrast to the 100% reactivity to 0.1 mg/ml wild-type HEV-VLP, although 0.1 mg/ml p18-VLP showed 100% reactivity to the antibody 447-52D. These results indicated a successful insertion of p18 peptide after residue Y485, which in turn disrupted the binding interface to antibody HEP224 but enabled the binding to 447-52D antibody.

2.2. The assembly of p18-VLP

The p18-VLP appeared as a spherical projection decorated with spikes on a surface profile (Fig. 2A). The projection image showed light density in the center, suggesting that the VLP was free of nucleic acid, like the wild-type HEV-VLP. The cryo-EM map revealed 30 protruding spikes positioned at each of the icosahedral two-fold axes (Fig. 3). Close investigation of the density radial distribution revealed several minor differences between p18- and HEV-VLPs. The density of the P domain appeared thicker in p18-VLP at a radius of 120 Å and two subunits appeared weakly associated than that in the wild-type VLP (Fig. 3). The density of p18-VLP at radius of 110 Å rotated slightly clockwise from that in the the wild type VLP, although the M-domain remained at the same orientation (r = 102 Å) in both VLPs. Thus, the insertion of p18 peptide did not interfere with VLP icosahedral base; instead it modified slightly the orientation of the P-domain. The coordinates of PORF2 subunits agreed well with the cryo-EM density map of p18-VLP (Fig. 4 A). No adjustment was needed to fine-tune the lateral contacts between subunits. The coordinates of three domains were in good consistence to the density of icosahedral shell, the threefold plateau, and the protruding spikes, except the flexible hinge loop between the M- and P-domains (Fig. 4B). Therefore, the chimeric PORF2 retained the tertiary and quaternary structure of HEV wild type VLP. Most notably, the P-domain demonstrated the same intermolecular contacts as the wild type, despite of local proteolytic cleavage in individual subunits.

2.3. Susceptibility to proteolytic digestion

The sequence of p18 peptide is rich in positively-charged amino acids and contains three arginines at positions I1, I4, and I8 as well as one lysine at position I15 (Fig. 1). Insertion of such a sequence in

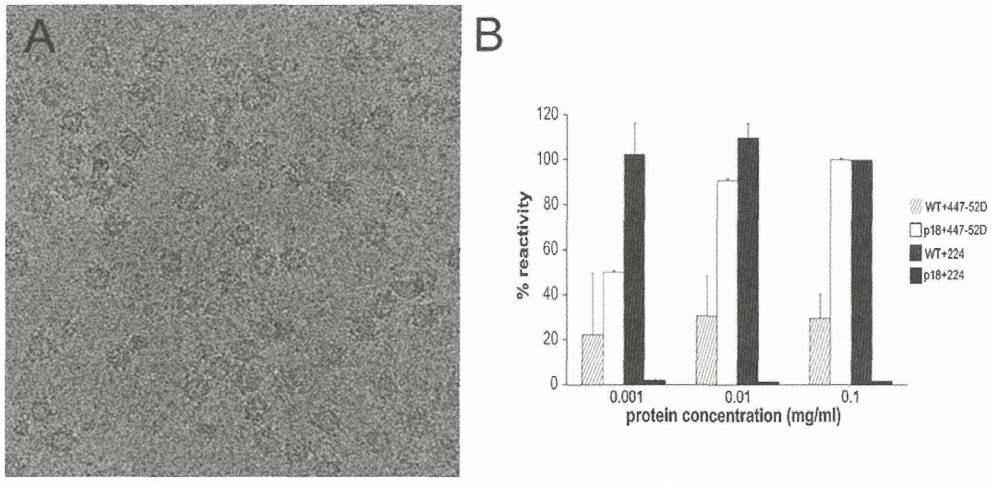

Fig. 2. The characterization of p18-VLPs. (A) Cryo-electron micrograph of frozen-hydrated p18-VLP. (B) Reactivity of antibodies HIV447-52D (white bars) and HEV224 (black bars) to the p18-VLPs (non-striated) and WT-VLPs (striated) as determined by ELISA. The data are averaged from triplicate experiments and are expressed as mean ± S.D. Note high immunoreactivity of p18-VLPs with anti-HIV447-52D but it is completely diminished with anti-HEV224.

the middle of a solvent-exposed region of a viral capsid may introduce vulnerable sites for trypsin cleavage, a feature that did not exist in the original protein. As tested by immunoblotting using anti-HIV-1 antibody 447-52D, a single immune-reactive band was detected at a position corresponding to a molecular weight of 53 kD from the samples purified in the presence of protease inhibitor (Fig. 5A). Without the protease inhibitor, a weakly immunoreactive band of 42 kD in molecular weight was observed from the sample collected at 6 days p.i., in addition to the 53 kDa band (Fig. 5A). Upon storage of 25 days in the absence of protease inhibitor, the intensity of the 42 kD peptide increased dramatically (Fig. 5A) in corresponding to the decrease of the 53 kD peptide. However, the intensity of the immune-reactive band at 42 kD remained undetectable if protease inhibitor was added (Fig. 5A). These results indicated possible protease cleavage and the cleavage may occur at the insertion region, most likely at the C-terminal end of p18 (I15) because the

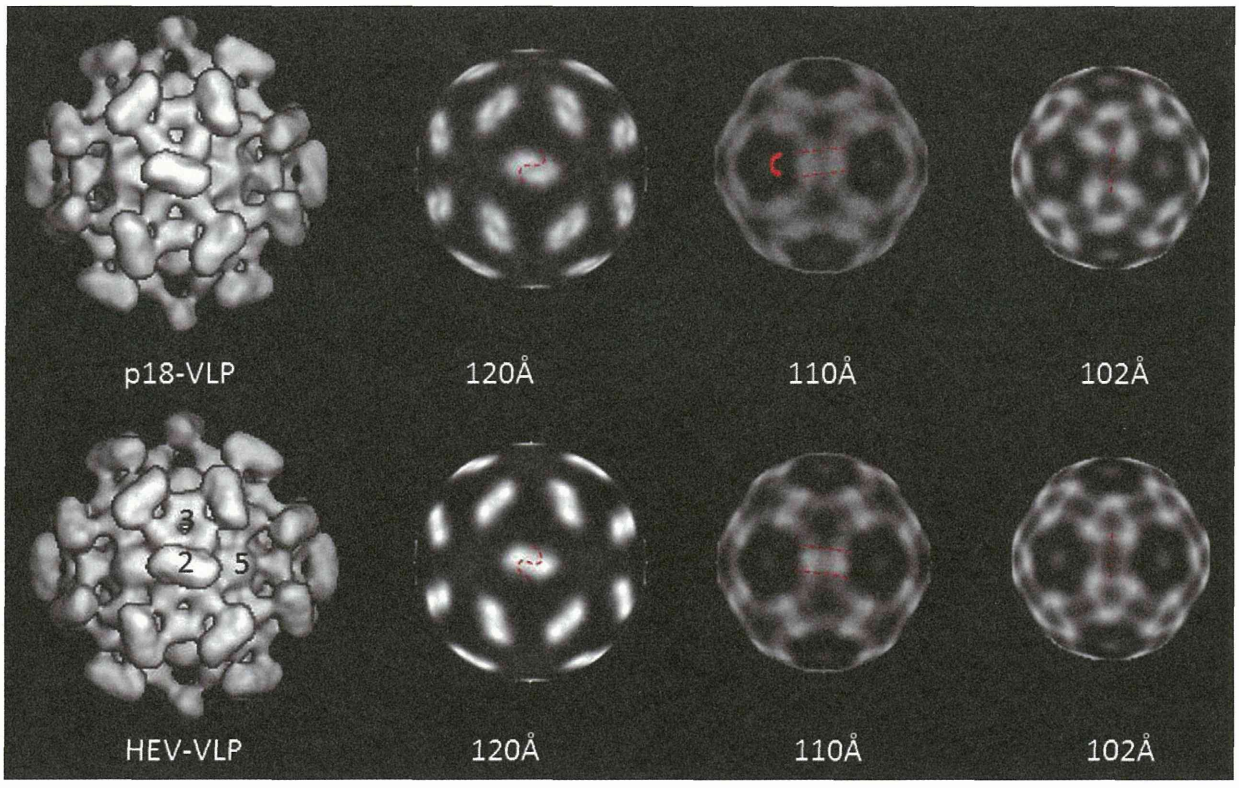

Fig. 3. Three-dimensional density maps of p18-VLP (top panel) and the wild type HEV-VLPs (bottom panel). The surface rendering map shows that the p18-VLP resembles the appearance of HEV-VLP and contains spike and plateau at 2fold- and 3-fold axes, respectively (the position of icosahedral axes is labeled with the corresponding number). The particles were sliced into thin sections to show the density distribution at radii of 120 Å (the P-domain), 110 Å (the M-domain) and the 102 Å (the S-domain). The red dashed lines profile the difference between the p18-VLP and the wild type HEV-VLP.

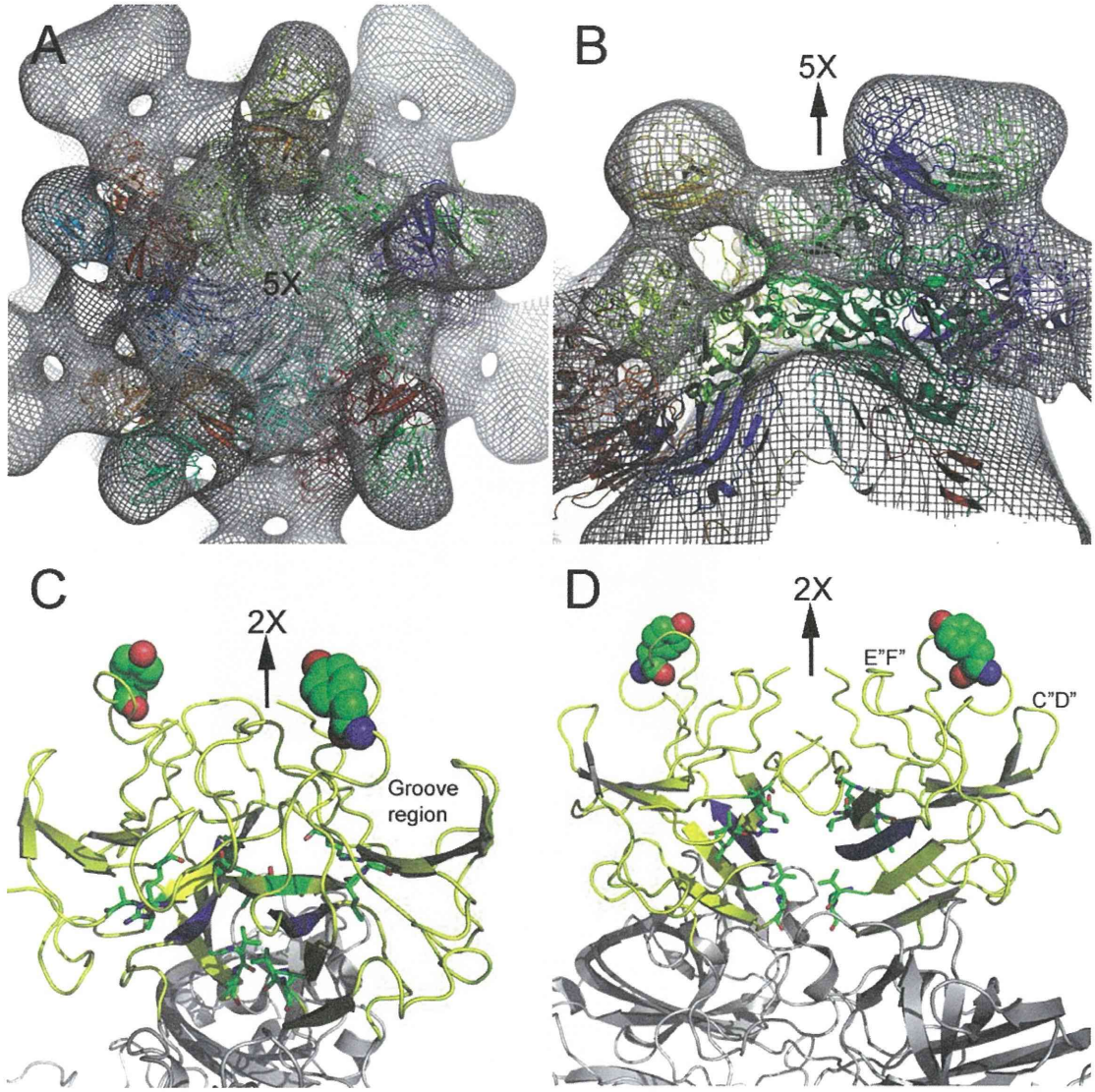

Fig. 4. Fitting of p18-VLP cryo-EM density map with the crystal structure of the HEV-VLP. The coordinates of PORF2 decamer (pentamer of dimers) agreed well with the cryo-EM density map at 5fold-axis region (A) and with the separation of S-, M- and P-domain (B). Ribbon presentation of a PORF2 dimer showing the position of surface groove region (C) and the hydrophobic residues (stick presentations) at the P-domain dimeric interface (D).

calculated mass of the fragment from residue 112–485 (40.5 kDa) agreed well with the measured one and the p18 immunogenicity is integrated with the 42 kDa fragment.

2.4. Resistance to trypsin and pepsin treatment

In order to test the stability of the chimeric VLPs in a highly proteolytic milieu, we further investigated the proteolytic digestion of the purified p18-VLPs with trypsin and pepsin, two enzymes that are present abundantly in the digestive tract. Because the 42 kD peptide remains immunoreactive with anti-HIV-1 antibody 447-52D, i.e. the enzyme cleavage site is most likely at the C-terminal end of the p18 insertion; therefore, trypsin is the dominant enzyme in this reaction. In the presence of trypsin, the 53 kDa band disappeared while the 42 kDa band remained unchanged (Fig. 5B). There was no extra band observed after silver staining. In contrast, the wild-type VLPs remained resistant to trypsin treatment (data not shown). Like trypsin, pepsin is an enzyme in stomach that cleaves peptide bonds between hydrophobic and preferably aromatic amino acids and did not enhance trypsin digestion of intact p18-VLP. After disassembly by the mixture of EDTA and DTT, the combination of trypsin and pepsin enhanced proteolytic digestion of PORF2 individual dimers. It further digested 42 kD peptide into short peptides of multiple lengths that appeared as extra bands in SDS-PAGE. We then investigated whether protease cleavage of p18-VLP disassembles the VLP structure. We then investigated whether protease cleavage disrupted the structure of p18-VLP. We treated p18-VLP with 30 mU/ml of trypsin for one hour and examined the treated p18-VLP via electron microscopy. The negatively stained p18-VLPs appeared as empty ring-like profiles covered with spikes (Fig. 5C). The measured diameter of the projection was ~25 nm, consistent with the diameter reported for the T = 1 HEV-VLP. Therefore, this data demonstrated that the p18-VLP maintained the VLP structure after proteolytic cleavage and retained the resistance to hydrolytic enzyme.

The structural integrity of p18-VLP is further demonstrated by the consistency between the structures of VLPs with and without p18 insertion (Fig. 4A and B). Therefore, the chimeric PORF2 retained the tertiary structure of properly folded PORF2, and assembled into a quaternary structure resembling the VLP of wild type in

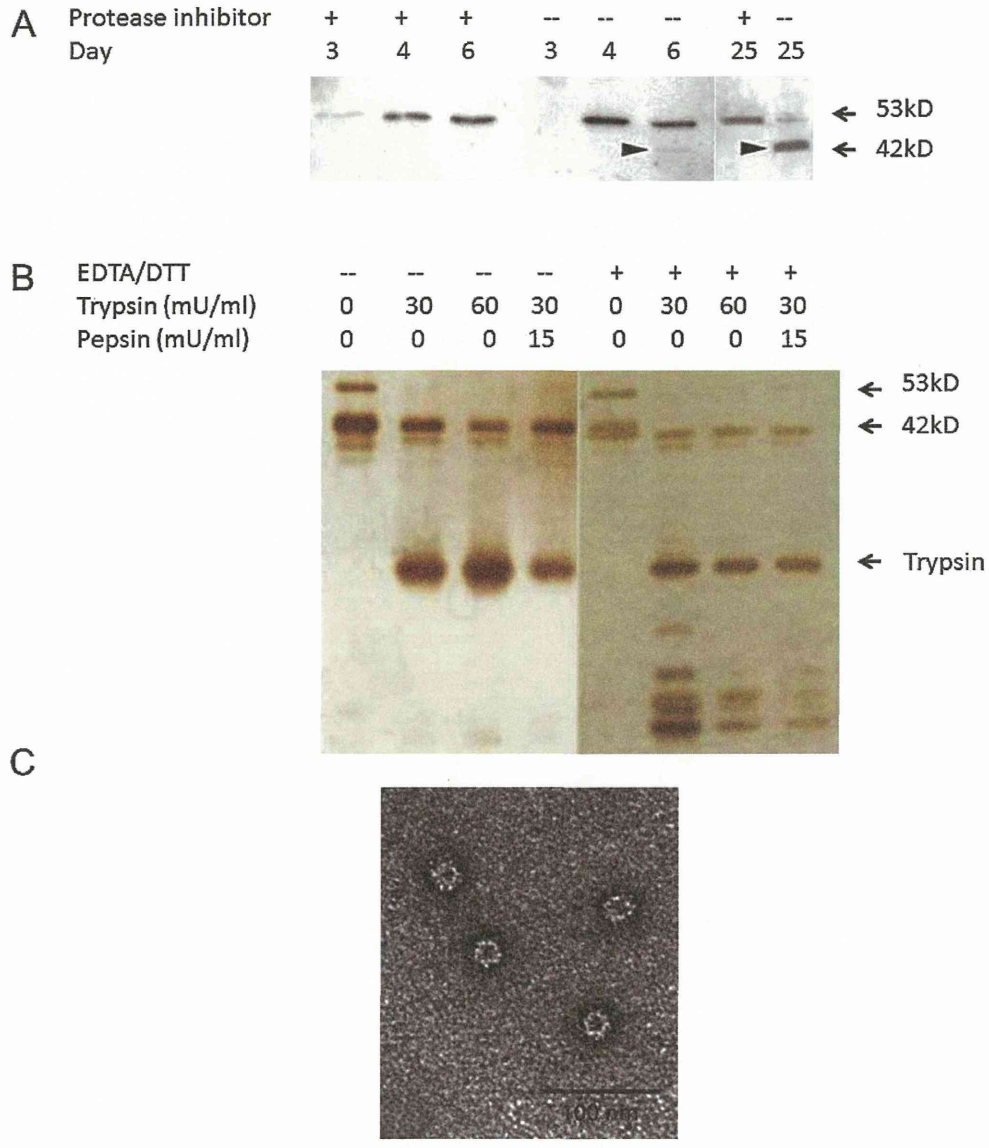

Fig. 5. Hydrolysis of the p18-VLPs. (A) VLPs recovered from the culture media in the presence (+)/absence (−) of protease inhibitors were subjected on SDS-PAGE under reducing condition and then immunoblotted with anti-HIV-1 antibody 447-52D. (B) Electrophoresis result of the p18-VLP pretreated with EDTA/DTT, 30 mU/ml or 60 mU/ml trypsin, and 15 mU/ml pepsin. The SDS-PAGE was performed under reducing condition and developed with silver staining. (C) Electron micrograph of negatively stained p18-VLPs after treatment with 60 mU trypsin. Bars = 100 nm.

the organization of domain display and the subunit contact. Most notably, the protruding spike of the p18-VLP remained in association as dimeric units on top of the intact icosahedral shell, despite of local proteolytic cleavage in individual subunits.

3. Discussion

Virus-like particles have gained increasing interest in vaccine development due to multiple reasons. The effect of their delivery depends largely on the insertion site where the foreign epitope can be well-integrated into VLP structure without causing interference with VLP assembly. The exposed terminus of the capsid protein is the common choice for such task. However, with a known crystal structure, a peptide insertion can be arranged at surface antigenic loop without disturbing the VLP structure to reduce the reactivity to the given antibodies.

The antigenic domain of HEV is reported as conformational and a handful of amino acids were determined as essential to antibody binding by mutagenesis [16,24]. They can be grouped as two surface patches located at the two opposite sides of the P-domain (Fig. 6A). The binding site of antibody HEP224 is composed of three surface loops around residue Tyr485 [22]. Insertion of p18 peptide at Tyr485 disrupted the interaction of these loops leading to conformational rearrangement. As a result, the newly defined the loop organization is no long complimentary to HEP224 paratope and inhibits the binding of other antibodies that recognize the same location as HEP224 (data not shown). Insertion of p18 peptide does not shield completely the antigenic domain; therefore further mutation is necessary to fully block the response of HEV-VLP to the pre-existing anti-HEV antibodies.

Trypsin cleavage did not eliminate the antigenicity of p18 when inserted after residue Y485, since the 42 kD peptide is immunoreactive to antibody 447-52D. This chimeric VLP can thus be used as vector to deliver protein antigen and more immunological experiment is necessary. However, the p18-peptide, when exposed on the surface of VLP by insertion at C-terminal end of PORF2, is

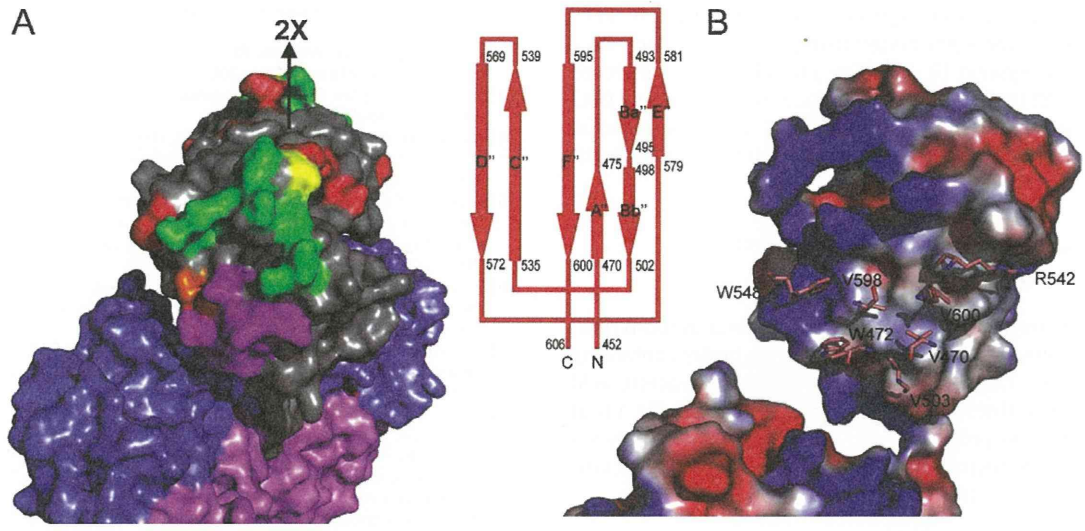

Fig. 6. Antigenic structure and dimeric interface of the P-domain. (A) Surface presentation of a HEV dimer, in which the P-, M-, and S-domain are colored in gray, slate blue, and light pink, respectively. The antibody-binding amino acids identified by mutagenesis are colored in the red. They overlap with HEP224 binding-site (green) at residue S487 (yellow) and with 8C11 binding-site (magenta) at residue D496 (colored in brown). (B) Surface potential representation of PORF2 mononer to show the dimeric contacting interface at the P-domain. The blue region is positively charged while the red region is negatively charge and the white region is non-polar. The amino acids of the ball-and-stick model are labelled to show residues that are critical for dimer formation. (For interpretation of the references to color in this figure legend, the reader is referred to the web version of the article.)

able to induce HIV-1 V3 loops specific antibody in mice (data not shown). Nevertheless, peptide remains surface-exposed to be recognized by the target molecules when inserted after residue Y485 of PORF2.

The three-dimensional reconstruction of the p18-VLP showed little difference to the structure of wild-type VLPs, even when subjected to an enzymatic environment. Trypsin cleavage most likely occurred at the C-terminal end (I15) of the inserted p18 peptide and did not induce spike disassociation from the icosahedral shell. This can be explained by the intermolecular forces of attraction that hold the quaternary structure of HEV-VLP (Fig. 6B). The hydrophobic effect is the primary weak force stabilizing the folding of the P-domain as well as its interaction between two P-domains within the same spike. There are 28 hydrophobic amino acids lining within the P-domains and five of them are from the β-strand A″ (amino acids 470-475) which is well protected by the β-sheet F″A″Bb″. The strong hydrophobic interactions hold the association of β-strand A″ to the C-terminal fragment after trypsin cleavage at residue I15 and tighten up the connection of the C-terminal fragment to icosahedral shell. Thus, the hydrophobic core of the P-domain actually protects p18-VLP integrity so that the VLP remained intact even in a proteolytic environment.

In conclusion, we reported a chimeric HEV-VLP that carried a foreign epitope at outermost surface that induces conformational changes at antigenic domain while maintains the tertiary and quaternary structures as well as the biological resistance to proteolytic enzymes. Moreover, the antigenic peptide can be replaced with a short peptide sequence. It has be reported that attachment to M cells at guts epithelium initiates antigen-specific mucosal immune responses [25] and that the α5β1 integrin is uniquely distributed on the apical surface of M cells but on the lateral and basolateral surfaces of neighboring enterocytes [26]. It is therefore possible to design a chimeric HEV-VLP carrying an Arg-Gly-Asp (RGD) integrin-binding motif to enhance M-cell uptake [27], and even carrying a targeting molecules to retarget HEV-VLP to particular cell types, e.g. RGD motif to retarget angiogenic endothelial cells by interacting with the overexpressed integrin receptors [28]. Angiogenesis, a process for the formation of new capillary blood vessels, has a crucial role in solid tumor progression and the development of metastasis. RGD-functionalized HEV-VLP therefore provides a safe and non-invasive vector for cancer antiangiogenic therapy, which is designed to arrest the growth or spread of tumors.

4. Materials and methods

4.1. Cloning of p18 sequence into position 485 of PORF2-HEV

To insert the HIV-1 p18 epitope into the PORF2 gene, the baculovirus transfer vector carrying the PORF2 gene (pFastBac1/PORF2-HEV/MluI) was mutated to create a unique *Mlu*I at the desired location. The QuikChange® Site-directed Mutagenesis Kit (Stratagene, La Jolla, CA) was used according to the manufacturer's instructions to change base pairs at position 1457 (G to C) and 1458 (C to G) so as to create an *Mlu*I restriction enzyme site that corresponds to position 485 in the protein sequence in PORF2-HEV. The mutagenesis primers HEVMluFwd (5′GACCAGTCCACTTACG**CG**TCTTCGACCGGCCCA3′) and HEVMluRev (5′TGGGCCGGTCGAAGACGCGTAAGTGGACTGGTC3′) were used for this purpose. This resulted in a relatively conservative Gly to Ala change at position 486 in PORF2. Positive clones were confirmed by screening plasmids for the presence of the newly created *Mlu*I restriction enzyme site (pFastBac1/PORF2-HEV/MluI) by *Mlu*I digestion.

Two overlapping phosphorylated oligonucleotides, p18pos#485Top (5′phos CGCGTCGCGTATCCAGAGGGGACCAGGGAGAGCATTTGTTACAATAGGAAAAGA) and p18pos#485Bottom (5′phos CGCGTCTTTTCCTATTGTAACAAATGCTCTCCCTGGTCCCCTCTGGATACGCGA 3′), encoding the p18 epitope sequence flanked by *Mlu*I ends, were annealed and ligated to *Mlu*I-digested pFastBac1/PORF2-HEV/MluI. Clones were screened for correct insertion and orientation by DNA sequencing (pFastBac1/PORF2-HEV/P18pos#485).

4.2. Production and purification of p18-VLP

The recombinant baculovirus vectors used to express VLPs bearing p18 epitopes were generated using the Bac-to-Bac® Baculovirus Expression System [8–10]. The p18-VLPs were collected and purified through multiple steps of ultracentrifugation and CsCl equilibrium density gradient. The purified p18-VLP was stored in 10 mM potassium-MES buffer (pH 6.0) in the presence/absence of protease inhibitors (1:50, v/v).

4.3. Enzymatic digestions of p18 HEV-VLPs and protein characterization

Proteolytic treatment was carried out for one hour at room temperature. Disassembly of p18-VLPs were done in a buffer containing 50 mM Tris–HCl (pH 7.5) 1 mM ethylene glycol tetra-acetic acid (EGTA), 20 mM dithiothreitol (DTT), and 150 mM NaCl for 1 h at room temperature. The products of cleavage were then analyzed by SDS-PAGE under reducing conditions and stained using a commercial silver staining kit from Invitrogen.

4.4. ELISA to detect binding to HEP 224 and 447-52D

The 96-well plate was coated with VLP and interacted with anti-HEV antibody HEP 224 and anti-HIV-1 antibody 447-52D. The antibody reaction was detected by alkaline phosphatase-labeled secondary antibodies and developed using p-nitrophenylphosphate solution.

4.5. Negative staining of proteolyzed p18-VLPs

The reaction mixtures were loaded onto a glow-discharged, carbon-coated EM grids and stained with 2% uranyl acetate. The samples were examined under a JEOL-1230 transmission electron microscope (TEM) and the images were recorded on a CCD camera (TVIPS Gauting, Germany) at a magnification of 40,000×.

4.6. Cryo-EM and three-dimensional image reconstruction

Cryo-EM and sample preparation were performed according to the previously described protocol [9]. The specimen was transferred into a JEOL 2100F TEM with a Gatan 626 cryo transfer system and the micrographs were recorded under a low-dose condition (<10 electrons/Å^2) on a TVIPS CCD camera at an interval of 2 Å at specimen space. Micrographs exhibiting minimal astigmatism and specimen drift were selected for image processing. The origin and orientation of each individual particle was first estimated and refined using a model-based polar Fourier transform (PFT) method [29,30]. The three-dimensional density map was computed with superimposing 5-3-2 icosahedral symmetry. The final density map was reconstructed from 945 individual particles with the final resolution at 15.3 Å assessed with Fourier shell correlation by taking correlation coefficient of 0.5 as cutoff. The fitting was carried out initially with program O [31] and refined Situs autofitting program [31–34] and was stopped when the cross correlation coefficient reached 80%. The final figures were generated using PyMOL [35].

Acknowledgment

The authors thank Dr. Tatsuo Miyamura for the supportive guidance. This study was funded by grants of NIH NCI pilot, NIH grant (AI095382) and UC Discovery Programs. PJ and WW were supported in part by a research grant from the Commission on Higher Education (CHE), and Faculty of Science at Mahidol University in Thailand.

References

[1] Holmgren J, Czerkinsky C. Mucosal immunity and vaccines. Nat Med 2005;11:S45–53.
[2] Ogra PL, Faden H, Welliver RC. Vaccination strategies for mucosal immune responses. Clin Microbiol Rev 2001;14:430–45.
[3] Ludwig C, Wagner R. Virus-like particles-universal molecular toolboxes. Curr Opin Biotechnol 2007;18:537–45.
[4] Uchida M, Klem MT, Allen M, Suci P, Flenniken M, Gillitzer E, et al. Biological containers: protein cages as multifunctional nanoplatforms. Adv Mater 2007;19:1025–42.
[5] Clark B, Caparros-Wanderley W, Musselwhite G, Kotecha M, Griffin BE. Immunity against both polyomavirus VP1 and a transgene product induced following intranasal delivery of VP1 pseudocapsid-DNA complexes. J Gen Virol 2001;82:2791–7.
[6] Tam AW, Smith MM, Guerra ME, Huang CC, Bradley DW, Fry KE, et al. Hepatitis E virus (HEV): molecular cloning and sequencing of the full-length viral genome. Virology 1991 Nov;185(1):120–31.
[7] Emerson S, Purcell R. Hepatitis E virus. In: Knipe DM, Howley PM, editors. Fields Virology. Fifth ed. Philadelphia: Lippincott Willimas & Wilkins; 2007. p. 3047–58.
[8] Li T-C, Takeda N, Miyamura T, Matsuura Y, Wang JCY, Engvall H, et al. Essential elements of the capsid protein for self-assembly into empty virus-like particles of hepatitis E virus. J Virol 2005;79(October (20)):12999–3006.
[9] Xing L, Kato K, Li T, Takeda N, Miyamura T, Hammar L, et al. Recombinant hepatitis E capsid protein self-assembles into a dual-domain T = 1 particle presenting native virus epitopes. Virology 1999;265(December (1)):35–45.
[10] Li TC, Yamakawa Y, Suzuki K, Tatsumi M, Razak MA, Uchida T, et al. Expression and self-assembly of empty virus-like particles of hepatitis E virus. J Virol 1997;71(October (10)):7207–13.
[11] Takamura S, Niikura M, Li TC, Takeda N, Kusagawa S, Takebe Y, et al. DNA vaccine-encapsulated virus-like particles derived from an orally transmissible virus stimulate mucosal and systemic immune responses by oral administration. Gene Ther 2004;11(April (7)):628–35.
[12] Niikura M, Takamura S, Kim G, Kawai S, Saijo M, Morikawa S, et al. Chimeric recombinant hepatitis E virus-like particles as an oral vaccine vehicle presenting foreign epitopes. Virology 2002;293(February (2)):273–80.
[13] Li T, Takeda N, Miyamura T. Oral administration of hepatitis E virus-like particles induces a systemic and mucosal immune response in mice. Vaccine 2001;19(May (25–26)):3476–84.
[14] Xing L, Li TC, Miyazaki N, Simon MN, Wall JS, Moore M, et al. Structure of hepatitis E virion-sized particle reveals an RNA-dependent viral assembly pathway. J Biol Chem 2010;285:33175–83.
[15] Guu T, Liu Z, Ye Q, Mata D, Li K, Yin C, et al. Structure of the hepatitis E virus-like particle suggests mechanisms for virus assembly and receptor binding. Proc Natl Acad Sci U S A 2009;106:12992–7.
[16] Yamashita T, Mori Y, Miyazaki N, Cheng H, Yoshimura M, Unno H, et al. Biological and immunological characterics of hepatitis E virus-like particles based on the crystal structure. Proc Natl Acad Sci U S A 2009;106:12986–91.
[17] Schofield DJ, Purcell RH, Nguyen HT, Emerson SU. Monoclonal antibodies that neutralize HEV recognize an antigenic site at the carboxyterminus of an ORF2 protein vaccine. Vaccine 2003;22(December (2)):257–67.
[18] Zhang J, Gu Y, Ge SX, Li S, He Z, Huang G, et al. Analysis of hepatitis E neutralization sites using monoclonal antibodies directed against a virus capsid protein. Vaccine 2005;23:2881–92.
[19] Li X, Zafrullah M, Ahmad F, Jameel S. A C-terminal hydrophobic region is required for homo-oligomerization of the hepatitis E virus capsid (ORF2) protein. J Biomed Biotechnol 2001;1(3):122–8.
[20] Li S, Tang S, Seetharaman J, Yang CY, Gu Y, Zhang J, et al. Dimerization of hepatitis E virus capsid protein E2s domain is essential for virus-host interaction. PLos Pathog 2009;5(8):e1000537.
[21] Yu H, Li S, Yang CY, Wei M, Song C, Zheng Z, et al. Homology model and potential virus-capsid binding site of a putative HEV receptor Grp78. J Mol Model 2010 [Epub ahead of print].
[22] Xing L, Wang JC, Li TC, Yasutomi Y, Lara J, Khudyakov Y, et al. Spatial configuration of hepatitis E virus antigenic domain. J Virol 2011;85(January (2)):1117–24.
[23] Takahashi H, Cohen J, Hosmalin A, Cease KB, Houghten R, Cornette JL, et al. An immunodominant epitope of the human immunodeficiency virus envelope glycoprotein gp160 recognized by class I major histocompatibility complex molecule-restricted murine ctyotoxic T lymphocytes. Proc Natl Acad Sci U S A 1988;85:3105–9.
[24] Zhou YH, Purcell R, Emerson S. A truncated ORF2 protein contains the most immunogenic site on ORF2: antibody responses to non-vaccine sequences following challenge of vaccinated and non-vaccinated macaques with hepatitis E virus. Vaccine 2005;23:3157–65.
[25] Kyd JM, Cripps A. Functional differences between M cells and enterocytes in sampling luminal antigens. Vaccine 2008;26:6221–4.
[26] Gullberg E, Keita AV, Salim SY, Andersson M, Caldwell KD, Söderholm JD, et al. Identification of cell adhesion molecules in the human follicle-associated epithelium that improves nanoparticle uptake into the Peyer's patches. J Pharmacol Exp Ther 2006;319(2):632–9.
[27] Clark M, Hirst BH, Jepson M. M-cell surface b1 integrin expression and invasin-mediated targetting of *Yersinia pseudotuberculosis* to mouse Peyer's patch M cells. Infect Immun 1998;66:1237–43.

[28] Ruoslahti E. RGD and other recognition sequences for integrins. Annu Rev Cell Dev Biol 1996;12:697–715.
[29] Baker TS, Cheng RH. A model-based approach for determining orientations of biological macromolecules imaged by cryoelectron microscopy. J Struct Biol 1996;116(January–February (1)):120–30.
[30] Baker TS, Cheng RH. A model-based approach for determining orientations of biological macromolecules imaged by cryoelectron microscopy. J Struct Biol 1996;116(1):120–30.
[31] Jones TA, Zou JY, Cowan SW, Kjeldgaard M. Improved method for building protein model in electron density maps and the location of errors in these models. Acta Crystallogr Sect A 1991;47:110–9.
[32] Wriggers W. Using situs for the integration of multi-resolution structures. Biophys Rev 2010;2:21–7.
[33] Xing L, Li TC, Mayazaki N, Simon MN, Wall JS, Moore M, et al. Structure of hepatitis E virion-sized particle reveals an RNA-dependent viral assembly pathway. J Biol Chem 2010;285(43):33175–83.
[34] Xing L, Wang JC, Li T-C, Yasutomi Y, Lara J, Khudyakov Y, et al. Spatial configuration of hepatitis E virus antigenic domain. J Virol 2011;85:1117–24.
[35] DeLano WL. The PYMOL molecular graphics system. Palo Alto, CA, USA: DeLano Scientific; 2002.

Veterinary Microbiology 163 (2013) 54–61

Contents lists available at SciVerse ScienceDirect

Veterinary Microbiology

journal homepage: www.elsevier.com/locate/vetmic

Susceptibility of laboratory rats against genotypes 1, 3, 4, and rat hepatitis E viruses

Tian-Cheng Li [a,*], Sayaka Yoshizaki [a], Yasushi Ami [b], Yuriko Suzaki [b], Shumpei P. Yasuda [c], Kumiko Yoshimatsu [c], Jiro Arikawa [c], Naokazu Takeda [d], Takaji Wakita [a]

[a] Department of Virology II, National Institute of Infectious Diseases, Gakuen 4-7-1, Musashi-murayama, Tokyo 208-0011, Japan
[b] Division of Experimental Animals Research, National Institute of Infectious Diseases, Gakuen 4-7-1, Musashi-murayama, Tokyo 208-0011, Japan
[c] Department of Microbiology, Graduate School of Medicine, Hokkaido University, Kita-15, Nishi-7, Kita-ku, Sapporo 060-8638, Japan
[d] Research Institute for Microbial Diseases, Osaka University, Suita, Osaka 565-0781, Japan

ARTICLE INFO

Article history:
Received 27 September 2012
Received in revised form 11 December 2012
Accepted 17 December 2012

Keywords:
Hepatitis E virus
Rat HEV
Laboratory rat
Wistar
Nude rat

ABSTRACT

To determine whether or not rats are susceptible to hepatitis E virus (HEV) infection, each of group containing three laboratory rats (Wistar) were experimentally inoculated with genotypes 1, 3, 4 and rat HEV by intravenous injection. Serum and stool samples were collected and used to detect HEV RNA and anti-HEV antibodies by RT-PCR and ELISA, respectively. The virus infection was monitored up to 3 months after inoculation. None of the serum or stool samples collected from the rats inoculated with G1, G3, or G4 HEV indicated positive sign for virus replication. Although no alteration was observed in ALT level, rat HEV RNA was detected in stools from both of the rats inoculated with rat HEV, and both rats were positive for anti-rat HEV IgG and IgM from 3 weeks after inoculation. These results demonstrated that rats are susceptible to rat HEV but not to G1, G3, and G4 HEV. We also confirm that the nude rats were useful for obtaining a large amount of rat HEV and that the rat HEV was transmitted by the fecal-oral route.

1. Introduction

Hepatitis E virus (HEV) is the sole member of the genus *Hepevirus* in the family *Hepeviridae* (Meng et al., 2012). HEV is a small round non-enveloped virus, 27–34 nm in diameter, containing an approximately 7.2 kb single-strand RNA molecule as the genome, which encodes three discontinuous and partially overlapping open reading frames (ORFs) (Balayan et al., 1983; Tam et al., 1991). The 5′ end of the RNA contains a cap structure, and the 3′ terminus of the RNA is polyadenylated (Kabrane-Lazizi et al., 1999b; Magden et al., 2001; Tam et al., 1991). HEV causes both epidemic and sporadic acute hepatitis E, which is not only a serious public health concern in many developing countries, but also is not rare among the general population in developed countries (Emerson and Purcell, 2003; Nelson et al., 2011). Pregnant women have a high mortality risk, as high as 20% (Khuroo et al., 1981; Navaneethan et al., 2008). HEV is transmitted primarily via the fecal-oral route through contaminated drinking water. The full genome of G1 HEV was first identified in 1990 (Reyes et al., 1990). Since then, a large number of HEV have been isolated from human and other animals (Meng et al., 1997; Nakamura et al., 2006; Tei et al., 2003; Zhao et al., 2009), and the HEV isolates were grouped into at least four major genotypes, genotypes 1–4 (G1–G4) on the basis of the nucleotide and deduced amino acid sequences (Liu et al., 2008). In addition to these four genotypes are mammalian HEV strains that have been isolated from wild boar, bat, avian, and wild rat (Drexler et al., 2012; Haqshenas et al., 2001; Johne et al., 2010a; Raj et al., 2012; Takahashi et al., 2011). Because G3 and G4 HEV were isolated from pigs and wild boars in addition to humans, and because much direct and indirect evidence has

* Corresponding author. Tel.: +81 42 561 0771; fax: +81 42 565 4729.
E-mail address: litc@nih.go.jp (T.-C. Li).

0378-1135/$ – see front matter © 2012 Elsevier B.V. All rights reserved.
http://dx.doi.org/10.1016/j.vetmic.2012.12.014

indicated that HEV is transmitted from pigs or wild boars to humans, hepatitis E is recognized as a zoonotic disease (Li et al., 2005; Meng, 2010).

Rat HEV was recently isolated from Norway rats in Germany (Johne et al., 2010a). However, the antigenicity, pathogenicity, and epidemiology of this virus remain unclear due to the lack of a viable cell culture system to grow the virus. Although anti-G1 HEV antibodies have been detected in wild rats in USA and Japan (Favorov et al., 2000; Hirano et al., 2003), it is obscure whether or not HEV (G1–G4 HEV, and wild boar HEV) substantially replicates in rats. Although it has been reported that G1, G2 and G3 HEV do not infect laboratory rats (Purcell et al., 2011), an early report showed that human HEV is transmissible to Wistar rats (Maneerat et al., 1996). Furthermore, part of the G3 HEV genome was detected recently in various species of wild-caught rats (Lack and Volk, 2012). At present, the susceptibility and infectivity of HEV in rat remain unclear. On the other hand, rat HEV-specific antibodies have been found in humans, suggesting the zoonotic potential of rat HEV (Dremsek et al., 2012). However, infection experiments indicated that monkey and pigs are not susceptible to rat HEV (Cossaboom et al., 2012; Purcell et al., 2011). In this study, we inoculated laboratory rats (Wistar) with G1, G3, G4, and rat HEV, and monitored the virus growth to determine the rats' susceptibility to HEV infection.

2. Materials and methods

2.1. Preparation of HEV

The G1 HEV strain was derived from stool specimens from a cynomolgus monkey (*Macaca fascicularis*), which had been experimentally infected with an Indian strain (Li et al., 2004). The G3 HEV strain (DQ079632) was derived from stool specimens collected on a pig farm in Japan. The G4 HEV strain (DQ079628) was from a stool specimen collected from a wild boar caught in Aichi prefecture, Japan. The infectivity of G1, G3, and G4 HEV had been confirmed by experimental infections with cynomolgus monkeys (Li et al., 2008). The copy numbers of the G1, G3, and G4 HEV genome in the stool specimens were 5×10^4, 2×10^4, and 1×10^5 per ml, respectively, by real-time RT-PCR as described previously (Jothikumar et al., 2006). Rat HEV (V-105) was derived from rat serum and lung tissue collected from a Vietnamese wild rat (Li et al., 2011). Because the rat serum was collected to detect anti-hantavirus antibodies, it was heat-inactivated at 56 °C for 30 min. The rat lung tissue was homogenized with 10 mM phosphate-buffered saline (PBS) to prepare a 10% suspension, shaken at 4 °C for 1 h, and clarified by centrifugation at 10,000 × *g* for 30 min. The supernatant was passed through a 0.45 μm membrane filter (Millipore, Bedford, MA). Both rat serum and lung suspensions were positive for rat HEV RNA by reverse-transcription polymerase chain reaction (RT-PCR); however, the amount of the rat HEV RNA was too low to be detected by real-time RT-PCR. All the specimens were stored at −80 °C until use.

2.2. Inoculation of rats and sample collection

Fifteen 5-week-old and six 20-week-old SPF rats (Wistar, Japan SLC), as well as two 5-week-old nude rats (Long–Evans-run/run, Japan SLC) were used in this study. All rats were female and negative for rat HEV RNA and anti-rat HEV antibodies, as determined by nested broad-spectrum RT-PCR and ELISA, respectively. To examine the laboratory rats' susceptibility to HEV, the rats were inoculated with HEV intravenously through the tail vein. To confirm the transmission route of rat HEV, two rats were fed in a cage in which had been placed 10 g of nude rats' stool samples containing 1.3×10^6 copy/g of rat HEV RNA. The rats were fed in the rat HEV-contaminated environment for one week and then moved to a new cage that was without rat HEV contamination. The serum samples were collected weekly for examining of HEV RNA as well as for HEV-specific IgG and IgM antibodies. Sera were also used to determine ALT values. Stool samples were collected daily after the inoculation to detect HEV RNA. Tissues of nude rats were collected after exsanguination, and a 10% tissue suspension was prepared as described above. The rats were monitored for 3–4 months after inoculation and were weighed daily. All the rat experiments were reviewed by the Institute's ethics committee and carried out according to the "Guides for animal experiments performed at NIID" under codes 111069 and 112011. Rats were individually housed in BSL-2 facilities.

2.3. A nested broad-spectrum RT-PCR

The RNA was extracted using the MagNA Pre LC system with MagNA Pre LC Total Nucleic Acid isolation (Roche Applied Science, Mannheim, Germany) according to the manufacturer's recommendations. Reverse transcription (RT) was performed at 42 °C for 50 min followed by 70 °C for 15 min in a 20 μl reaction mixture containing 1 μl of Superscript™ II RNase H⁻ reverse transcriptase (Invitrogen, Carlsbad, CA), 1 μl of the oligo(dT) primer, 1 μl of RNaseOUT™, 2 μl of 0.1 M dithiothreitol, 4 μl of 5 × RT buffer, 1 μl of 10 mM deoxynucleoside triphosphates, 5 μl of RNA, and 5 μl of distilled water.

A nested broad-spectrum RT-PCR analysis was performed to amplify a portion of the ORF1 genome, based on the method described previously with slight modification (Johne et al., 2010b). Five microliters of the cDNA was used for the first PCR in 50 μl of the reaction mixture containing an external forward primer, HEV-cs (5′-TCGCGCATCACMTTYTTCCARAA-3′), and an external reverse primer, HEV-cas (5′-GCCATGTTCCAGACDGTRTTCCA-3′). Each cycle consisted of denaturation at 95 °C for 30 s, primer annealing at 52 °C for 45 s, and an extension reaction at 72 °C for 60 s followed by final extension at 72 °C for 7 min. Two microliters of the first PCR product were used for the nested PCR with an internal forward primer, HEV-csn (5′-TGTGCTCTGTTTGGCCCNTGGTTYCDG-3′), and an internal reverse primer, HEV-casn (5′-CCAGGCTCACCRGARTGYTTCTTCCA-3′). Each cycle consisted of denaturation at 95 °C for 30 s, primer annealing at 55 °C for 45 s, and an extension reaction at 72 °C for 60 s followed by final

extension at 72 °C for 7 min. The nested PCR products were separated by electrophoresis on 2% agarose gels.

2.4. Quantitative real-time RT-PCR for detection of rat HEV

To determine rat HEV RNA titers, a TaqMan assay was performed by using the 7500 FAST Real-Time PCR System (Applied Biosystems, Foster City, CA, USA) according to the manufacturer's recommendations. The primers consisted of 900 nmol/L forward (5′-GTGGTGCTTTTATGGTGACTG-3′, nt 4123–4143) and 900 nmol/L reverse (5′-CAAACTCAC-TAAAATCATTCTCAAACAC-3′, nt 4196–4223), and 250 nmol/L probe (5′-6FAM-GTTCAGGAGAAGTTC-GAGGCCGCCGT-TAMRA-3′, nt 4148–4173). One-step quantitative RT-PCR (qRT-PCR) cycling conditions were 15 min at 48 °C, a 10-min incubation at 95 °C, and 50 cycles for 15 s at 95 °C and 1 min at 60 °C. Standard RNA is a partial genome of V-105 (nt 3991–5100) that was synthesized by using the MEGA script kit (Applied Biosystems). A 10-fold serial dilution of standard RNA (10^7 to 10^1 copies) was used for the quantitation of viral copy numbers in reaction tubes. Amplification data were collected and analyzed with Sequence Detector software version 1.3 (Applied Biosystems). This quantitative real-time RT-PCR system, with a sensitivity of 10 copies, was used exclusively for rat HEV.

2.5. Detection of IgG and IgM antibodies

Anti-rat HEV IgG and IgM antibodies were detected by enzyme-linked immunosorbent assay (ELISA) as described previously (Li et al., 2011). Flat-bottom 96-well polystyrene microplates (Immulon 2; Dynex Technologies, Chantilly, VA) were coated with the purified rat HEV-LPs (1 μg/mL, 100 μl/well) and incubated overnight at 4 °C. The unbound HEV-LPs were removed, and the plates were washed twice with 10 mM phosphate-buffered saline containing 0.05% Tween 20 (PBS-T) and then blocked with 200 μl of 5% skim milk (Difco Laboratories) dissolved in PBS-T for 1 h at 37 °C. After the plates were washed four times with PBS-T, diluted rat (100 μl/well) serum samples were added in duplicate. The plates were incubated at 37 °C for 1 h and washed three times as described above. The wells were incubated with 100 μl of horseradish peroxidase-conjugated goat anti-rat IgG (H+L) (Zemed Laboratories, San Francisco, CA) (1:10,000 dilution) or horseradish peroxidase-conjugated goat anti-rat IgM (Jackson Immunoresearch Laboratories Inc., West Grove, PA) (1:100,000 dilution), diluted with PBS-T containing 1% skim milk. The plates were incubated at 37 °C for 1 h and washed four times with PBS-T. The substrate orthophenylenediamine (100 μl) (Sigma Chemical, St. Louis, MO) and H_2O_2 were added to each well. The plates were incubated in a dark room at room temperature for 30 min, and then 50 μl of 4 N H_2SO_4 was added to each well. Absorbance was measured at 492 nm. The cutoff values for IgG and IgM were determined as described previously (Li et al., 2011). A sample was considered positive when the absorbance exceeded the cutoff value. Anti-G1, G3, and G4 HEV IgG and IgM antibodies were detected by ELISA as described previously (Li et al., 2000).

2.6. Liver enzyme level

ALT value was monitored weekly by the Fuji Dri-Chem Slide GPT/ALT-PIII kit (Fujifilm, Saitama, Japan). The geometric mean ALT during the pre-inoculation period of each animal was used as the normal ALT value, and a two-fold or greater increase at the peak was considered a sign of hepatitis.

3. Results

3.1. Rats became infected with rat HEV but not with G1, G3, or G4 HEV

Fifteen 5-week-old SPF rats (Wistar) were randomly assigned to five groups (Table 1). RT-PCR and ELISA indicated that all animals were negative for HEV RNA and anti-rat HEV antibodies prior to inoculation. All rats were inoculated intravenously with 300 μl of each sample. The rats in groups 1, 2, and 3 were inoculated with the stool samples containing 10^4 copies of G1, G3, and G4 HEV, respectively. Two rats in group 4 and two in group 5 were inoculated similarly with 10% rat lung homogenate or RNA-positive rat serum, respectively. Rat-12 and Rat-15 received PBS and were used to monitor the fecal-oral transmission of the virus (Table 1).

In groups 1, 2, 3, and 5, all the rat serum samples collected from 1 to 13 weeks p.i. were negative for HEV RNA, anti-HEV IgG, and anti-HEV IgM antibodies. ALT elevation was not observed in these serum samples. Consistent with the above results, HEV RNA was not detected in stool samples in those groups (data not shown). These results indicated that G1, G3, and G4 HEV as well as heat-inactivated rat HEV were unable to infect laboratory rats.

In contrast, anti-rat HEV IgG and IgM antibodies were detected in Rat-10 and Rat-11 at 4 and 5 weeks p.i. in group 4 (Fig. 1). The IgG titers increased with time, peaking at 10 and 7 weeks p.i. in Rat-10 and Rat-11, respectively, before gradually decreasing. The RNA was detected in the stool

Table 1
Grouping of HEV inoculation.

Groups	Rat no.	Genotype	Specimens	Virus titers
Group 1	Rat-1	G1 HEV	Monkey stool	10^4
	Rat-2	G1 HEV	Monkey stool	10^4
	Rat-3	G1 HEV	Monkey stool	10^4
Group 2	Rat-4	G3 HEV	Pig stool	10^4
	Rat-5	G3 HEV	Pig stool	10^4
	Rat-6	G3 HEV	Pig stool	10^4
Group 3	Rat-7	G4 HEV	Wild boar stool	10^4
	Rat-8	G4 HEV	Wild boar stool	10^4
	Rat-9	G4 HEV	Wild boar stool	10^4
Group 4	Rat-10	Rat HEV	Rat lung tissue	ND[a]
	Rat-11	Rat HEV	Rat lung tissue	ND[a]
	Rat-12	–	PBS	–
Group 5	Rat-13	Rat HEV	Rat serum[b]	ND[a]
	Rat-14	Rat HEV	Rat serum[b]	ND[a]
	Rat-15	–	PBS	–

[a] Less than detection threshold.
[b] Headed at 56 °C for 30 min.

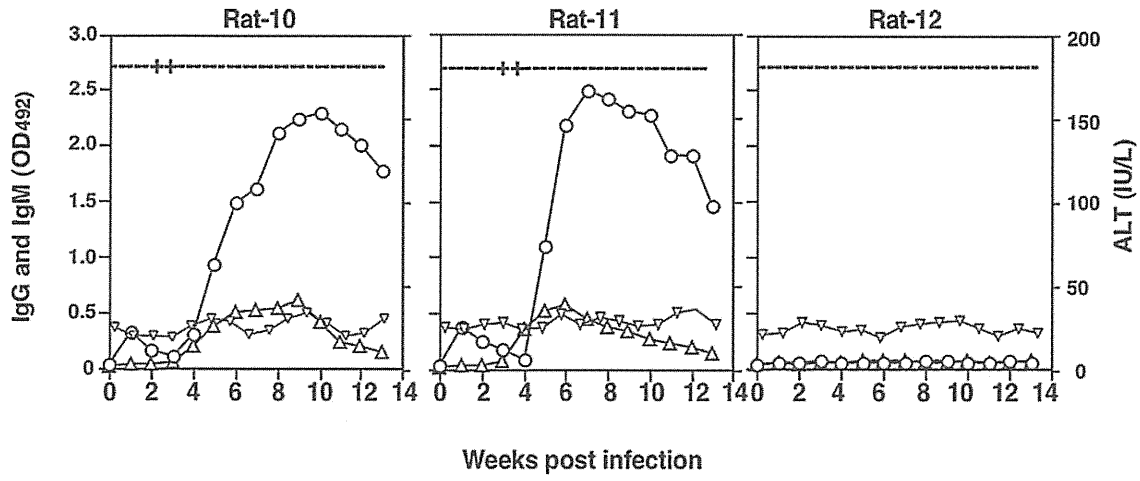

Fig. 1. Kinetics of biochemical, serological, and virological markers after intravenous inoculation. Laboratory rats (Wistar) were inoculated with rat HEV-positive lung suspension (Rats 10 and 11) or PBS (Rat-12). HEV RNA in the stool was monitored by RT-PCR: +, positive; −, negative. Anti-rat HEV IgG (○) and IgM (△) antibodies were detected by ELISA, and ALT (▽) elevation was monitored.

specimens from Rat-10 on days 17–20 and from Rat-11 on days 21–24 p.i. The copy numbers of the RNA were low and were detectable only by the nested RT-PCR (data not shown). Rat HEV RNA was undetectable in the rat serum. The nucleotide sequences of the amplified products from the stool specimens were identical to those detected from the lung suspension samples (data not shown). These results demonstrated that rat HEV is infectious to laboratory rats.

During the 3 months of the experiments, the ALT levels of all the rats were lower than 40 IU/L, demonstrating no changes in liver failure. The body weights of the infected rats increased similarly to those without infection, even in the period when rat HEV replication was extensive. No virus replication markers were detected in one of the non-inoculated rat (Rat-15). In this case, we found no evidence of oral transmission of rat HEV.

3.2. Infectivity of stools recovered from V-105-infected rats

To confirm the infectivity of rat HEV recovered from Rat-10 and Rat-11, stool samples taken from Rat-10 on day 18 p.i. and those from Rat-11 on day 22 p.i. were made to 10% stool suspensions. Two 20-week-old female rats (Rat-10a and Rat-10b) were intravenously inoculated with 300 μl of the suspension from Rat-10. Similarly, Rat-11a and Rat-11b were used for the stool suspension from Rat-11. As shown in Fig. 2, anti-rat HEV IgG and IgM antibodies were detected in the sera from all four rats at 3 weeks p.i. Rat HEV RNA was detected in stool from three of the rats, Rat-10a, Rat-10b, and Rat-11a, indicating that the rat HEV recovered from laboratory rats Rat-10 and Rat-11 are infectious. The ALT level did not increase during the experiment in any of the four rats (data not shown).

Because serum and stools recovered from laboratory rats contain extremely low copy numbers of rat HEV, two 5-week-old nude rats (athymic rats), NR1 and NR2, were intravenously injected with 300 μl of a 10% stool suspension derived from Rat-10 to produce a larger amount of rat HEV. In both nude rats, viral RNA was first detected at 3 weeks p.i. in sera and at 2 weeks p.i. in the stool (Fig. 3). The RNA increased, peaking at 12 weeks in serum with titers 1.6×10^3 copy/ml, and were constantly detected in feces with the titers 2×10^6–7×10^6 copy/g. The IgG was negative during the experimental period (data not shown).

To compare the viral loads in different tissues of the nude rats, the sera, intestinal contents, and tissues including liver, heart, spleen, lung, kidney, bladder, womb, salivary gland, and muscle were collected following the exsanguination at the 120 days p.i. The viral RNA titers were detected by real-time RT-PCR with a 10% suspension of each tissue or 100 μl of blood. In addition to the intestinal contents, high virus titers were observed in the liver: 3.1×10^7 and 3.9×10^7 copies/g in nude rats N1 and N2, respectively (Fig. 4). Other than the liver, the spleen was the only other site where HEV RNA was detected, with an extremely low titer, 2.1×10^2, suggesting that rat HEV replicates in liver and is secreted in intestine.

3.3. Rat HEV transmitted through fecal-oral route

Because human HEV is transmitted via a fecal-oral route, the possibility of the same transmission route was examined. Two 20-week-old female rats, OR1 and OR2, were fed in a cage with 10 g of stool samples containing 1.3×10^6 copy/g of rat HEV RNA derived from rat HEV-infected nude rats N1 and N2. After one week, both rats were moved to a clean cage and serum and stool samples were collected to monitor the RNA.

As shown in Fig. 5, rat HEV RNA in stools was detected from 36 to 42 days p.i. in OR1 and from 13 to 20 days p.i in OR2. Anti-rat HEV IgG and IgM were both detected in the sera at 6 and 3 weeks p.i. in OR1 and OR2, respectively. The IgM antibody titers peaked at 7 and 5 weeks p.i. then decreased gradually. The IgG antibody titers peaked at 8 and 5 weeks, respectively, and remained at high levels until the end of the experiment. Rat HEV RNA in the serum samples was detected at 3 weeks p.i. only in OR2. These results indicated that rat HEV was transmitted through the fecal-oral route. Compared with intravenous inoculation, transmission by the fecal-oral route took more time and higher titers of rat HEV to establish infection. The anti-IgG

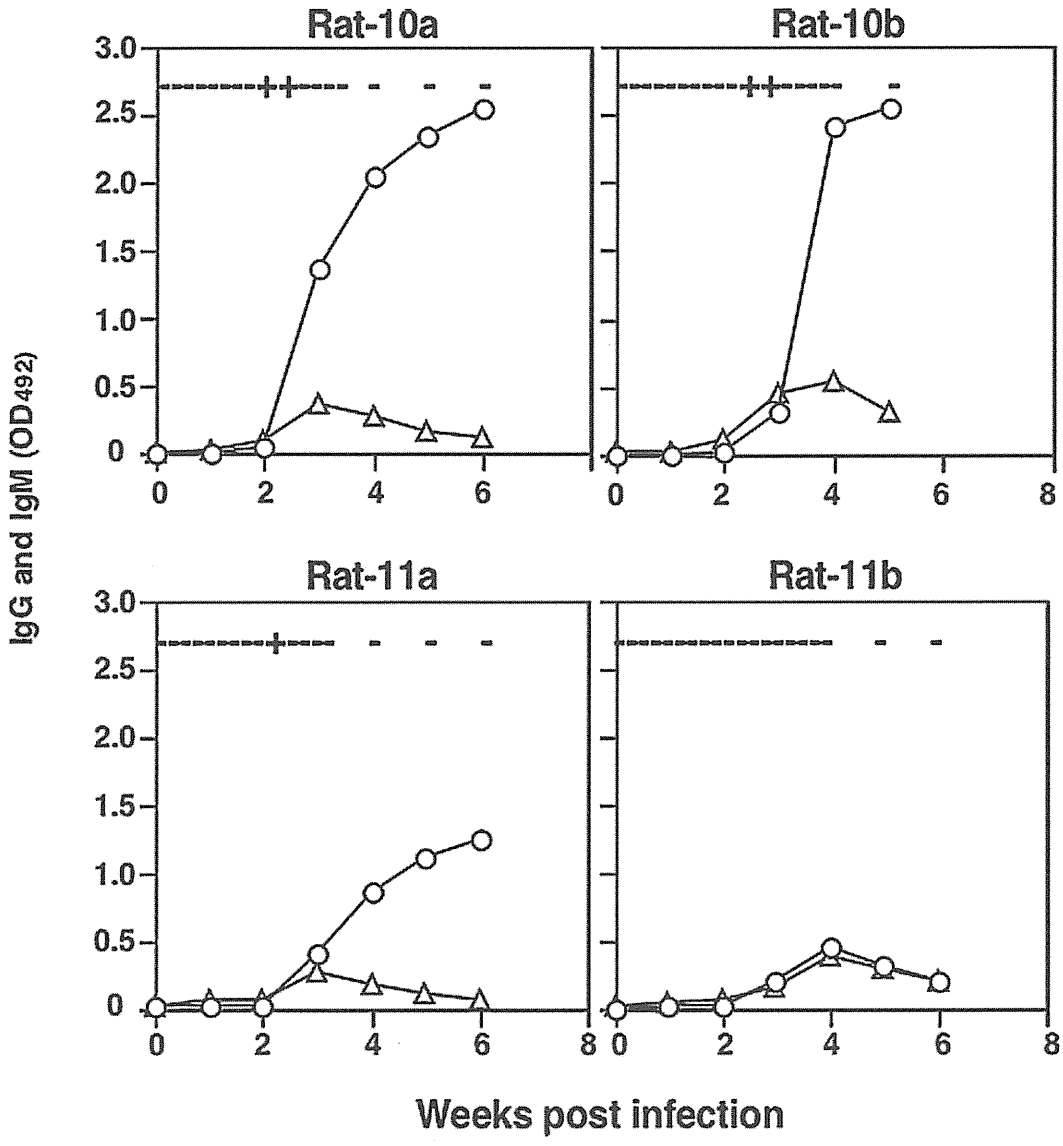

Fig. 2. Infectivity of the stool suspensions derived from the V-105-infected rats. Laboratory rats (Rats 10a and 10b) were inoculated with the stool suspension from Rat-10. Stool samples were collected daily and serum samples were collected weekly until 6 or 8 weeks. Similarly, Rats 11a and 11b were inoculated with the stool suspension from Rat-11. HEV RNA in the stool was monitored by RT-PCR: +, positive; −, negative. Serum IgG (○) and IgM (△) antibodies were detected by ELISA.

antibody induced by oral inoculation lasted longer than that induced by intravenous inoculation.

4. Discussion

Rats have long been suspected as a potential reservoir for HEV. Before rat HEV was isolated in Germany, anti-HEV IgG antibodies have been detected in various rat species, including Norway (*Rattus norvegicus*), black (*Rattus rattus*), and cotton (*Sigmodon hispidus*) rats (Arankalle et al., 2001; Favorov et al., 2000; Hirano et al., 2003; Kabrane-Lazizi et al., 1999a) by using the antigens derived from G1 HEV, suggesting that HEV or HEV-like virus infection occurred in wild rats. However, the source of the infection was confirmed in a few cases, and it is not clear whether the anti-HEV IgG was induced by HEV or other HEV-like viruses. In 2002, it was reported that the partial genome of the genotype 1 HEV was detected from wild rats in Nepal (He et al., 2002). However, that paper was retracted in 2006 because of a suspicion that the Nepal rodent HEV sequence was contaminated in the laboratory.

Recently, the capsid proteins of rat HEV were expressed by a recombinant baculovirus in insect Tn5 cells; these proteins were found to be self-assembled and to form virus-like particles (V-LPs). An ELISA was developed using rat HEV-LPs as antigens and was employed to examine the rat HEV-specific IgG and IgM responses. We found that 20.9% and 3.6% of wild rats in Vietnam were positive for rat HEV IgG and IgM antibodies, respectively. Furthermore, a new rat HEV strain, V-105, was isolated from rat HEV IgM-positive serum (Li et al., 2011).

To determine whether or not rat HEV can infect laboratory rats and to examine the susceptibility of laboratory rats to other HEV genotypes, we performed infection experiments using G1, G3, G4, and rat HEV with laboratory rats. No sign of viral replication of G1, G3, or G4

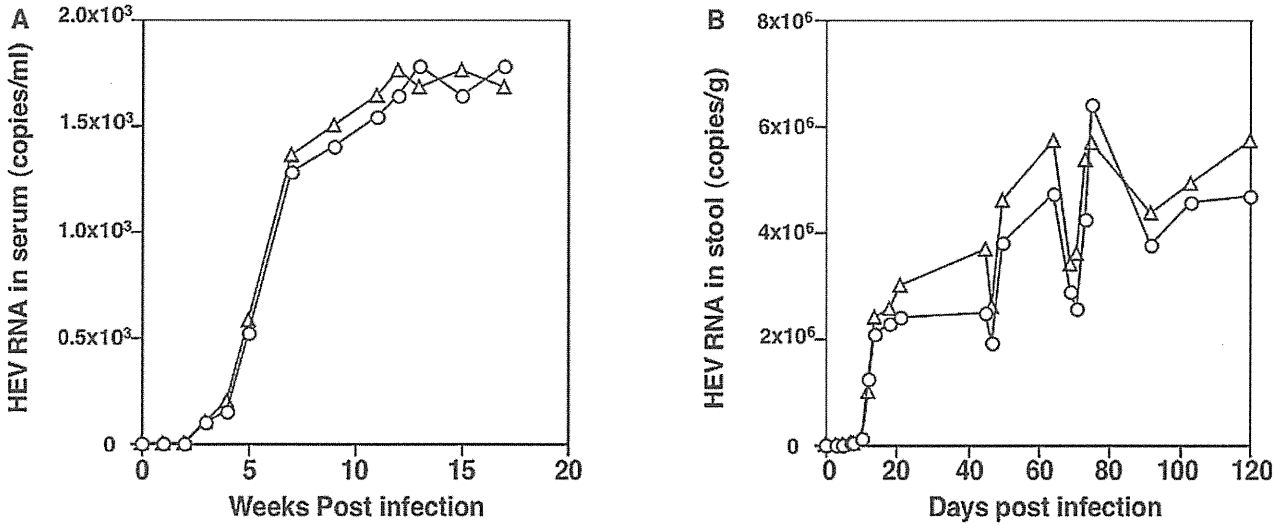

Fig. 3. Kinetics of rat HEV RNA in nude rats. Two nude rats were intravenously inoculated with rat HEV-containing stool suspension. HEV RNA in the serum (A) and stool (B) were monitored by real-time RT-PCR. Nude rat N1, ○; nude rat N2, △.

HEV was observed, and we concluded that the laboratory rats were resistant to G1, G3, and G4 HEV infection. Therefore, the anti-HEV IgG antibodies reported in various species of rats before may be cross-reactive antibodies induced by HEV or HEV-like virus other than human HEV. This result was consistent with that reported by Purcell et al., in which they confirmed that genotype 1. 2 and 3 HEV do not infect laboratory rats (Purcell et al., 2011). However, Maneerat et al. (1996) published a contradictory result, in which it has reported that human HEV (presumably genotype 1) was transmissible to Wistar laboratory rats, although others have not been able to reproduce this report. Recently Lack and Volk (2012) isolated strains of genotype 3 HEV from various species of wild-caught rats in the United States. Although the detailed sequences data are not available, the genetic trees from the Technical Appendix shows that isolated sequences are quite similar to those of G3 HEV strain AF082843, isolated from a pig in the United States. However, this strain failed to infect to laboratory rats (Purcell et al., 2011).

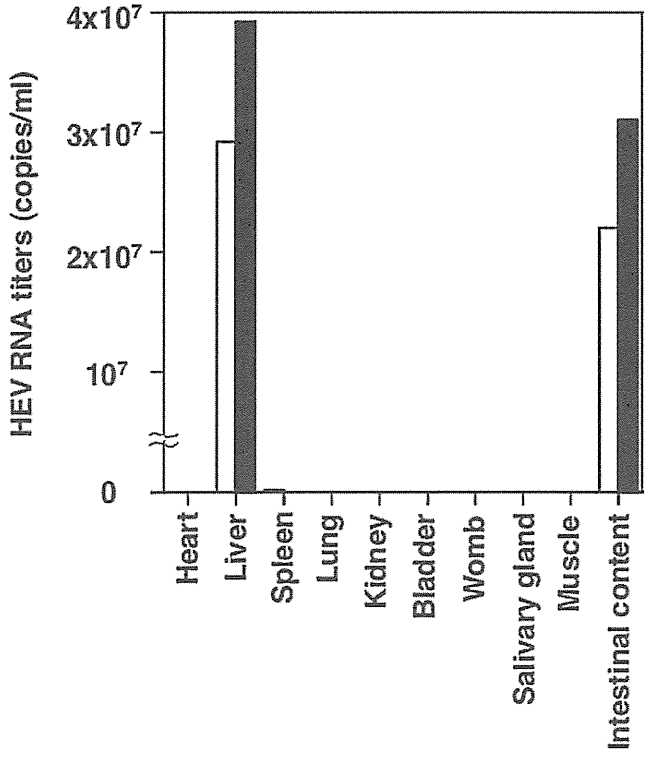

Fig. 4. Distribution of rat HEV in a nude rat. HEV RNA in different tissues from two nude rats, NR1 (white bars) and NR2 (black bars), are shown.

In contrast to G1, G3, and G4 HEV, HEV derived from wild rats infected the laboratory rats. Although no rat HEV RNA was detected in the serum samples, seroconversions were observed and rat HEV was detected in stool, demonstrating that laboratory rats are susceptible to rat HEV. We also confirmed that rat HEV was transmitted by the fecal-oral route. However, during the experimental period, rat weight increased as with normal rats and the ALT level did not change (Fig. 1). These results suggested that rat HEV, at least in low doses, might not be pathogenic to rats, as shown in this study, where i.v. inoculation or oral transmission did not induce any serious sign in the rats. We also found that the infectivity of rat HEV was lost after heat treatment at 56 °C for 30 min, suggesting that rat HEV can be inactivated relatively easily.

Because the wild rat serum has been heated at 56 °C for 30 min, we used rat lung homogenates containing rat HEV RNA to inoculate laboratory rats for the transmission study. We did not think rat HEV could be replicated at lung tissues, and we think that rat HEV RNA is included in the blood remaining in the lung tissues. In fact, after exsanguinations, the lung tissues from experimentally infected nude rats were all negative for HEV RNA. In addition, rat HEV RNA was not detected in heart, spleen, kidney, bladder, womb, salivary gland, or muscle, though it was detected in liver, suggesting that rat HEV replicates in rat liver.

In this study we confirmed that rat HEV infection was transmitted through the fecal-oral route. However, rat R-12 did not become infected with rat HEV (Fig. 1) even

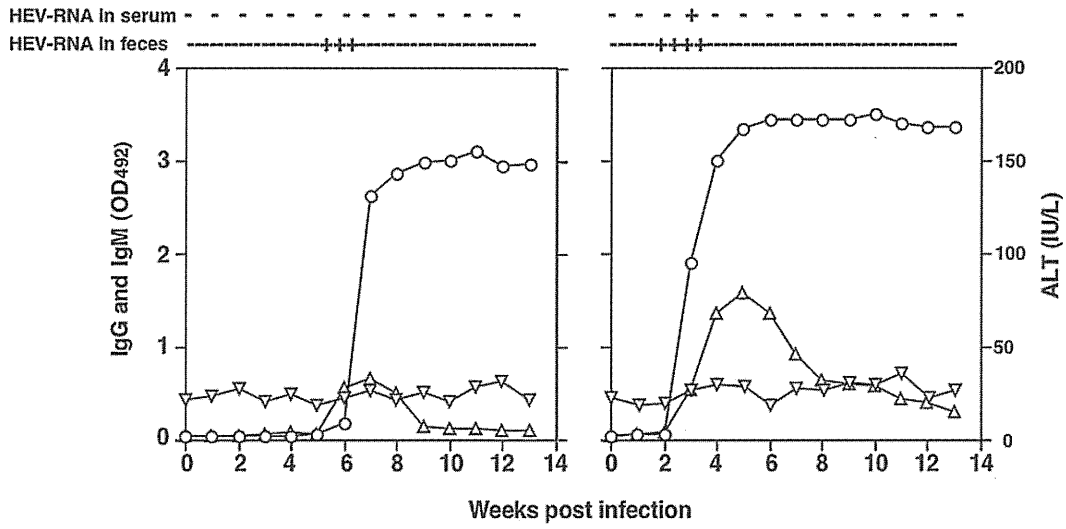

Fig. 5. Kinetics of biochemical, serological, and virological markers after oral inoculation. Laboratory rats were fed HEV-contaminated food for one week, and then viral RNA in the sera and stool were monitored by RT-PCR; +, positive; −, negative. Anti-rat HEV IgG (○) and IgM (△) antibodies were detected by ELISA, and ALT (▽) elevation was monitored.

though it was kept with HEV-infected rats, R-10 and R-11. The amount of rat HEV in the stools was too low to cause infection. Thus, HEV infection by oral inoculation may require more virus than that by intravenous inoculation. Our results clearly showed that the nude rats were useful to obtain a large amount of virus for further study of the cell culture and characterization of rat HEV.

When IgG antibody kinetics were compared between intravenous inoculation and oral inoculation, we found that oral inoculation induced higher titers, which was maintained for a long time without decline (Fig. 5). These results give us a hint about the route of HEV vaccination. Thus far, phase II and III recombinant HEV vaccine trials have been reported by two research groups (Shrestha et al., 2007; Zhu et al., 2010). Both groups delivered the candidate HEV vaccine by intramuscular injection. Although the protective efficacy against clinically overt HEV infection was confirmed, the duration of protection afforded by this vaccine remains unknown. Shrestha et al. (2007) reported that only 56.3% of vaccine inoculators maintained a level of anti-HEV antibody for 2 years post-vaccination. As natural HEV infection occurs via the fecal-oral route, oral delivery of an HEV vaccine could induce the same immune responses as natural infection. It is necessary to consider whether the oral delivery of HEV vaccine induces immune responses that are stronger than those induced by intramuscular inoculation.

Conflict of interest statement

None declared.

Acknowledgments

This study was supported in part by grants for Research on Emerging and Re-emerging Infectious Diseases, Research on Hepatitis, and Research on Food Safety from the Ministry of Health, Labor, and Welfare, Japan.

References

Arankalle, V.A., Joshi, M.V., Kulkarni, A.M., Gandhe, S.S., Chobe, L.P., Rautmare, S.S., Mishra, A.C., Padbidri, V.S., 2001. Prevalence of anti-hepatitis E virus antibodies in different Indian animal species. J. Viral Hepat. 8, 223–227.

Balayan, M.S., Andjaparidze, A.G., Savinskaya, S.S., Ketiladze, E.S., Braginsky, D.M., Savinov, A.P., Poleschuk, V.F., 1983. Evidence for a virus in non-A, non-B hepatitis transmitted via the fecal-oral route. Intervirology 20, 23–31.

Cossaboom, C.M., Cordoba, L., Sanford, B.J., Pineyro, P., Kenney, S.P., Dryman, B.A., Wang, Y., Meng, X.J., 2012. Cross-species infection of pigs with a novel rabbit, but not rat, strain of hepatitis E virus isolated in the United States. J. Gen. Virol. 93, 1687–1695.

Dremsek, P., Wenzel, J.J., Johne, R., Ziller, M., Hofmann, J., Groschup, M.H., Werdermann, S., Mohn, U., Dorn, S., Motz, M., Mertens, M., Jilg, W., Ulrich, R.G., 2012. Seroprevalence study in forestry workers from eastern Germany using novel genotype 3- and rat hepatitis E virus-specific immunoglobulin G ELISAs. Med. Microbiol. Immunol. 201, 189–200.

Drexler, J.F., Seelen, A., Corman, V.M., Fumie Tateno, A., Cottontail, V., Melim Zerbinati, R., Gloza-Rausch, F., Klose, S.M., Adu-Sarkodie, Y., Oppong, S.K., Kalko, E.K., Osterman, A., Rasche, A., Adam, A., Muller, M.A., Ulrich, R.G., Leroy, E.M., Lukashev, A.N., Drosten, C., 2012. Bats worldwide carry hepatitis E virus-related viruses that form a putative novel genus within the family Hepeviridae. J. Virol. 86, 9134–9147.

Emerson, S.U., Purcell, R.H., 2003. Hepatitis E virus. Rev. Med. Virol. 13, 145–154.

Favorov, M.O., Kosoy, M.Y., Tsarev, S.A., Childs, J.E., Margolis, H.S., 2000. Prevalence of antibody to hepatitis E virus among rodents in the United States. J. Infect. Dis. 181, 449–455.

Haqshenas, G., Shivaprasad, H.L., Woolcock, P.R., Read, D.H., Meng, X.J., 2001. Genetic identification and characterization of a novel virus related to human hepatitis E virus from chickens with hepatitis-splenomegaly syndrome in the United States. J. Gen. Virol. 82, 2449–2462.

He, J., Innis, B.L., Shrestha, M.P., Clayson, E.T., Scott, R.M., Linthicum, K.J., Musser, G.G., Gigliotti, S.C., Binn, L.N., Kuschner, R.A., Vaughn, D.W., 2002. Evidence that rodents are a reservoir of hepatitis E virus for humans in Nepal. J. Clin. Microbiol. 40, 4493–4498.

Hirano, M., Ding, X., Li, T.C., Takeda, N., Kawabata, H., Koizumi, N., Kadosaka, T., Goto, I., Masuzawa, T., Nakamura, M., Taira, K., Kuroki, T., Tanikawa, T., Watanabe, H., Abe, K., 2003. Evidence for widespread infection of hepatitis E virus among wild rats in Japan. Hepatol. Res. 27, 1–5.

Johne, R., Heckel, G., Plenge-Bönig, A., Kindler, E., Maresch, C., Reetz, J., Schielke, A., Ulrich, R.G., 2010a. Novel hepatitis E virus genotype in Norway rats, Germany. Emerg. Infect. Dis. 16, 1452–1455.

Johne, R., Plenge-Bonig, A., Hess, M., Ulrich, R.G., Reetz, J., Schielke, A., 2010b. Detection of a novel hepatitis E-like virus in faeces of wild rats using a nested broad-spectrum RT-PCR. J. Gen. Virol. 91, 750–758.

Jothikumar, N., Cromeans, T.L., Robertson, B.H., Meng, X.J., Hill, V.R., 2006. A broadly reactive one-step real-time RT-PCR assay for rapid and sensitive detection of hepatitis E virus. J. Virol. Methods 131, 65–71.

Kabrane-Lazizi, Y., Fine, J.B., Elm, J., Glass, G.E., Higa, H., Diwan, A., Gibbs Jr., C.J., Meng, X.J., Emerson, S.U., Purcell, R.H., 1999a. Evidence for widespread infection of wild rats with hepatitis E virus in the United States. Am. J. Trop. Med. Hyg. 61, 331–335.

Kabrane-Lazizi, Y., Meng, X.J., Purcell, R.H., Emerson, S.U., 1999b. Evidence that the genomic RNA of hepatitis E virus is capped. J. Virol. 73, 8848–8850.

Khuroo, M.S., Teli, M.R., Skidmore, S., Sofi, M.A., Khuroo, M.I., 1981. Incidence and severity of viral hepatitis in pregnancy. Am. J. Med. 70, 252–255.

Lack, J.B., Volk, K., Van Den Bussche, R.A., 2012. Hepatitis E virus genotype 3 in wild rats, United States. Emerg. Infect. Dis. 18, 1268–1273.

Li, T.C., Chijiwa, K., Sera, N., Ishibashi, T., Etoh, Y., Shinohara, Y., Kurata, Y., Ishida, M., Sakamoto, S., Takeda, N., Miyamura, T., 2005. Hepatitis E virus transmission from wild boar meat. Emerg. Infect. Dis. 11, 1958–1960.

Li, T.C., Suzaki, Y., Ami, Y., Dhole, T.N., Miyamura, T., Takeda, N., 2004. Protection of cynomolgus monkeys against HEV infection by oral administration of recombinant hepatitis E virus-like particles. Vaccine 22, 370–377.

Li, T.C., Suzaki, Y., Ami, Y., Tsunemitsu, H., Miyamura, T., Takeda, N., 2008. Mice are not susceptible to hepatitis E virus infection. J. Vet. Med. Sci. 70, 1359–1362.

Li, T.C., Yoshimatsu, K., Yasuda, S.P., Arikawa, J., Koma, T., Kataoka, M., Ami, Y., Suzaki, Y., Mai le, T.Q., Hoa, N.T., Yamashiro, T., Hasebe, F., Takeda, N., Wakita, T., 2011. Characterization of self-assembled virus-like particles of rat hepatitis E virus generated by recombinant baculoviruses. J. Gen. Virol. 92, 2830–2837.

Li, T.C., Zhang, J., Shinzawa, H., Ishibashi, M., Sata, M., Mast, E.E., Kim, K., Miyamura, T., Takeda, N., 2000. Empty virus-like particle-based enzyme-linked immunosorbent assay for antibodies to hepatitis E virus. J. Med. Virol. 62, 327–333.

Liu, Z., Meng, J., Sun, X., 2008. A novel feature-based method for whole genome phylogenetic analysis without alignment: application to HEV genotyping and subtyping. Biochem. Biophys. Res. Commun. 368, 223–230.

Magden, J., Takeda, N., Li, T., Auvinen, P., Ahola, T., Miyamura, T., Merits, A., Kaariainen, L., 2001. Virus-specific mRNA capping enzyme encoded by hepatitis E virus. J. Virol. 75, 6249–6255.

Maneerat, Y., Clayson, E.T., Myint, K.S., Young, G.D., Innis, B.L., 1996. Experimental infection of the laboratory rat with the hepatitis E virus. J. Med. Virol. 48, 121–128.

Meng, X.J., 2010. Hepatitis E virus: animal reservoirs and zoonotic risk. Vet. Microbiol. 140, 256–265.

Meng, X.J., Anderson, D.A., Arankalle, V.A., Emerson, S.U., Harrison, T.J., Jameel, S., Okamoto, H., 2012. Hepeviridae. In: King, A.M.Q.A.M.J., Carstens, E.B., Lefkowitz, E.J. (Eds.), Virus Taxonomy: Ninth Report of the ICTV. Elsevier/Academic Press, London, pp. 1021–1028.

Meng, X.J., Purcell, R.H., Halbur, P.G., Lehman, J.R., Webb, D.M., Tsareva, T.S., Haynes, J.S., Thacker, B.J., Emerson, S.U., 1997. A novel virus in swine is closely related to the human hepatitis E virus. Proc. Natl. Acad. Sci. U. S. A. 94, 9860–9865.

Nakamura, M., Takahashi, K., Taira, K., Taira, M., Ohno, A., Sakugawa, H., Arai, M., Mishiro, S., 2006. Hepatitis E virus infection in wild mongooses of Okinawa, Japan: demonstration of anti-HEV antibodies and a full-genome nucleotide sequence. Hepatol. Res. 34, 137–140.

Navaneethan, U., Al Mohajer, M., Shata, M.T., 2008. Hepatitis E and pregnancy: understanding the pathogenesis. Liver Int. 28, 1190–1199.

Nelson, K.E., Kmush, B., Labrique, A.B., 2011. The epidemiology of hepatitis E virus infections in developed countries and among immunocompromised patients. Expert Rev. Anti. Infect. Ther. 9, 1133–1148.

Purcell, R.H., Engle, R.E., Rood, M.P., Kabrane-Lazizi, Y., Nguyen, H.T., Govindarajan, S., St Claire, M., Emerson, S.U., 2011. Hepatitis E virus in rats, Los Angeles, California, USA. Emerg. Infect. Dis. 17, 2216–2222.

Raj, V.S., Smits, S.L., Pas, S.D., Provacia, L.B., Moorman-Roest, H., Osterhaus, A.D., Haagmans, B.L., 2012. Novel hepatitis e virus in ferrets, the Netherlands. Emerg. Infect. Dis. 18, 1369–1370.

Reyes, G.R., Purdy, M.A., Kim, J.P., Luk, K.C., Young, L.M., Fry, K.E., Bradley, D.W., 1990. Isolation of a cDNA from the virus responsible for enterically transmitted non-A, non-B hepatitis. Science 247, 1335–1339.

Shrestha, M.P., Scott, R.M., Joshi, D.M., Mammen Jr., M.P., Thapa, G.B., Thapa, N., Myint, K.S., Fourneau, M., Kuschner, R.A., Shrestha, S.K., David, M.P., Seriwatana, J., Vaughn, D.W., Safary, A., Endy, T.P., Innis, B.L., 2007. Safety and efficacy of a recombinant hepatitis E vaccine. N. Engl. J. Med. 356, 895–903.

Takahashi, M., Nishizawa, T., Sato, H., Sato, Y., Jirintai, Nagashima, S., Okamoto, H., 2011. Analysis of the full-length genome of a hepatitis E virus isolate obtained from a wild boar in Japan that is classifiable into a novel genotype. J. Gen. Virol. 92, 902–908.

Tam, A.W., Smith, M.M., Guerra, M.E., Huang, C.C., Bradley, D.W., Fry, K.E., Reyes, G.R., 1991. Hepatitis E virus (HEV): molecular cloning and sequencing of the full-length viral genome. Virology 185, 120–131.

Tei, S., Kitajima, N., Takahashi, K., Mishiro, S., 2003. Zoonotic transmission of hepatitis E virus from deer to human beings. Lancet 362, 371–373.

Zhao, C., Ma, Z., Harrison, T.J., Feng, R., Zhang, C., Qiao, Z., Fan, J., Ma, H., Li, M., Song, A., Wang, Y., 2009. A novel genotype of hepatitis E virus prevalent among farmed rabbits in China. J. Med. Virol. 81, 1371–1379.

Zhu, F.C., Zhang, J., Zhang, X.F., Zhou, C., Wang, Z.Z., Huang, S.J., Wang, H., Yang, C.L., Jiang, H.M., Cai, J.P., Wang, Y.J., Ai, X., Hu, Y.M., Tang, Q., Yao, X., Yan, Q., Xian, Y.L., Wu, T., Li, Y.M., Miao, J., Ng, M.H., Shih, J.W., Xia, N.S., 2010. Efficacy and safety of a recombinant hepatitis E vaccine in healthy adults: a large-scale, randomised, double-blind placebo-controlled, phase 3 trial. Lancet 376, 895–902.

Epidemiol. Infect., Page 1 of 9. © Cambridge University Press 2012
doi:10.1017/S0950268812002385

A survey of rodent-borne pathogens carried by wild *Rattus* spp. in Northern Vietnam

T. KOMA[1], K. YOSHIMATSU[1], S. P. YASUDA[1], T. LI[2], T. AMADA[1], K. SHIMIZU[1], R. ISOZUMI[1], L. T. Q. MAI[3], N. T. HOA[3], V. NGUYEN[4], T. YAMASHIRO[5,6], F. HASEBE[7] AND J. ARIKAWA[1]*

[1] *Department of Microbiology, Graduate School of Medicine, Hokkaido University, Japan*
[2] *Department of Virology 2, National Institute of Infectious Diseases, Japan*
[3] *National Institute of Hygiene and Epidemiology, Hanoi, Vietnam*
[4] *Centre for International Health Quarantine, Hai Phong City, Hai Phong, Vietnam*
[5] *Institute of Tropical Medicine, Nagasaki University, Japan*
[6] *Vietnam Research Station, Nagasaki University, Japan Initiative for Global Research Network on Infectious Diseases (J-GRID)*
[7] *Centre of International Collaborative Research, Nagasaki University, Japan*

Received 8 May 2012; Final revision 11 September 2012; Accepted 4 October 2012

SUMMARY

To examine the prevalence of human pathogens carried by rats in urban areas in Hanoi and Hai Phong, Vietnam, we live-trapped 100 rats in January 2011 and screened them for a panel of bacteria and viruses. Antibodies against *Leptospira interrogans* (22·0%), Seoul virus (14·0%) and rat hepatitis E virus (23·0%) were detected in rats, but antibodies against *Yersinia pestis* were not detected. Antibodies against *L. interrogans* and Seoul virus were found only in adult rats. In contrast, antibodies to rat hepatitis E virus were also found in juvenile and sub-adult rats, indicating that the transmission mode of rat hepatitis E virus is different from that of *L. interrogans* and Seoul virus. Moreover, phylogenetic analyses of the S and M segments of Seoul viruses found in *Rattus norvegicus* showed that Seoul viruses from Hai Phong and Hanoi formed different clades. Human exposure to these pathogens has become a significant public health concern.

Key words: Hantavirus, hepatitis E, leptospirosis, surveillance, zoonoses.

INTRODUCTION

Rodents play a role as reservoir hosts of causative agents for various bacterial, viral and parasitic zoonoses. Wild rats (*Rattus* spp.) are a particularly important source of human pathogens because they inhabit areas in the vicinity of human dwellings.

* Author for correspondence: Professor J. Arikawa, Department of Microbiology, Graduate School of Medicine, Hokkaido University, Kita-ku, Kita-15, Nishi-7, Sapporo 060–8638, Japan. (Email: j_arika@med.hokudai.ac.jp)

Leptospirosis is caused by spirochaetes belonging to the genus *Leptospira*. Leptospirosis is an important worldwide zoonosis for which the major reservoir animals are rodents. Although some leptospirosis cases have been diagnosed correctly, leptospirosis is thought to be a major cause of undiagnosed acute febrile illness (AFI) in endemic countries [1]. About 12 outer membrane proteins, including LipL32, OmpL1, Ligb, LenA, LenD and Loa22, have been identified [2]. The major outer membrane lipoprotein, LipL32, is the most abundant protein of the entire cell and is highly conserved in pathogenic *Leptospira* spp. [3].

Hantavirus infection, haemorrhagic fever with renal syndrome (HFRS) and hantavirus pulmonary syndrome (HPS) are also known as worldwide rodent-borne viral zoonoses. Hantaviruses are enveloped and negative-sense RNA viruses with a tripartite genome comprising of large (L), medium (M) and small (S) segments [4]. Seoul virus (SEOV) is one of the causative agents of HFRS and is carried by *Rattus norvegicus*. We previously conducted epidemiological studies on the prevalence of SEOV infection in rodents and AFI patients who were not leptospirosis patients in East Asian countries including Vietnam [5, 6], Indonesia (Ibrahim *et al.*, unpublished data), Thailand [7], and Sri Lanka [8]. The epidemiological results indicate that SEOV infection exists in rodents and non-leptospirosis patients in all of those countries. However, hantavirus antibody-positive rates in non-leptospirosis AFI patients were about 2·3%, which is almost the same as the rate in healthy people in Vietnam [5]. Therefore, although SEOV infection is one of the possible causes of AFI, other causative agents are thought to exist.

Hepatitis E virus (HEV) is a positive-sense, single-stranded RNA virus, and the HEV genome includes two short non-coding regions surrounding three open reading frames (ORF1–ORF3). HEV can generally be divided phylogenetically into four genotypes. A genetically distinct HEV has recently been isolated from rats [9]. Our previous study showed the prevalence of rat HEV antibody in wild rats in Hanoi, Vietnam. Furthermore, the rat HEV genome was seen to be closely associated with rat HEV in Germany [10]. Although a recent study provided evidence of human infection with rat HEV in Germany [11], the relationship between rat HEV and human disease is still unclear.

In this study, we investigated the prevalence of *Leptospira interrogans*, SEOV and rat HEV in urban rats captured in urban areas in Hai Phong and Hanoi City, which are the second and third most populous cities in Vietnam, respectively. Antibody against *Yersinia pestis* was also examined as it is an important rodent-borne pathogen.

METHODS

Animals

Two hundred and 220 tomahawk live-traps were set in the evening and checked in the morning after a trapping night in residential districts of urban areas in Hanoi City (+105·84° E, 20·97° N) and inside a warehouse facing the residential district of an urban area in Hai Phong Port (+106·69° E, 20·87° N), in Northern Vietnam in January 2011. A total of 100 small mammals (94 *R. norvegicus*, 6 *R. tanezumi*) were captured in Hanoi City and in Hai Phong Port. Weight, sex and species identification were recorded for each animal. Species were identified by external morphology and DNA sequencing of the mitochondrial cytochrome *b* gene as described previously [5, 12]. Sequence data for cytochrome *b* obtained in this study were deposited in DDBJ/EMBL/GenBank (accession numbers: AB674753–AB674758, AB746356–AB746367). To investigate the relationship between maturation stage and seroprevalence, *R. norvegicus* were tentatively categorized by weight as juveniles (<100 g), sub-adults (100–200 g) and adults (>200 g) [13]. A blood sample was collected from each rodent via cardiac puncture under ether anaesthesia. Serum specimens were stored at −80 °C until serological examination. Lung specimens were collected and stored at −80 °C for polymerase chain reaction (PCR) examination of the hantavirus genome.

Antibody detection

Antibody against *L. interrogans* was detected by an enzyme-linked immunosorbent assay (ELISA) with *Escherichia coli*-expressed LipL32 of *L. interrogans* as an antigen according to a previously described method [14]. ELISA was performed essentially by the same procedure as described previously for hantavirus infection [15]. Briefly, wells of a 96-well plate were coated with 1 μg/ml antigen in phosphate-buffered saline (PBS). The plates were then blocked with PBS containing 3% bovine serum albumin (BSA) for 1 h at 37 °C. Rodent sera were diluted 1:200 with ELISA buffer (PBS containing 0·5% BSA and 0·05% Tween-20) and added to the wells. After incubation for 1 h at room temperature, the plates were washed three times with ELISA buffer, and horseradish peroxidase-conjugated goat anti-rat IgG antibody (Zymed Laboratories Inc., USA) was added as the secondary antibody. After incubation for 1 h at room temperature, the plates were washed as described above and colorimetric reaction was developed by the addition of *o*-phenylenediamine dihydrochloride (OPD; Sigma-Aldrich, USA). Optical density (OD) was measured at 450 nm. A negative antigen that included the Nus-tag protein, made from the pET43b

vector, was used as a negative control. The sample OD was calculated by subtracting the average OD for each set of negative antigen duplicates from the average OD for each set of LipL32 duplicates. Serum samples from three wild rats (*R. norvegicus*), which had been confirmed as antibody-negative to *L. interrogans* by various diagnoses, were used as negative control sera. The negative control sera were examined in all ELISA experiments, and mean OD value plus three times the standard deviations (S.D.) was used as a cut-off value to distinguish ELISA-positive and ELISA-negative samples. Antibody-positive sera were then subjected to Western blotting (WB) using the same antigen by the procedure described previously [16]. Samples were considered *L. interrogans* IgG antibody-positive if they were positive by both ELISA and WB.

Antibody to SEOV was detected by IgG ELISA with *E. coli*-expressed N-terminal 103 amino acids of the nucleocapsid protein as an antigen (HS103) as described previously [7]. Wells of a 96-well plate were coated with 1 μg/ml HS103 in PBS as a capture antigen. ELISA using HS103 antigen was performed using the same procedure as described above. Antibody-positive sera were then subjected to WB using the baculovirus-expressed antigen using the same procedure as described above [17]. Samples were considered SEOV IgG antibody positive if they were positive by both ELISA and WB.

Antibody to rat HEV was detected by ELISA with virus-like particles consisting of baculovirus-expressed rat HEV ORF2 proteins as described previously [10]. Wells of a 96-well plate were coated with 1 μg/ml rat HEV ORF2 proteins in PBS as a capture antigen. ELISA was then performed essentially by the same procedure as described above. However, blocking was performed using 5% skimmed milk dissolved in PBS-T for 1 h at 37 °C.

Antibody to *Y. pestis* was detected by ELISA with Fraction 1 antigen, which is a capsule-like antigen encoded by the *caf1* gene, as described previously [18]. Wells of a 96-well plate were coated with 1 μg/ml Fraction 1 antigen in PBS as a capture antigen. ELISA was then performed using the same procedure as described above.

Molecular characterization of hantaviruses

Total RNA was extracted from lung tissues of all *R. norvegicus* and *R. tanezumi* rodents using Isogen (Nippon Gene, Japan) and then reverse-transcribed using a First-Strand cDNA Synthesis kit (GE Healthcare UK Ltd, UK). Real-time PCR followed by PCR for sequencing of the hantavirus genome were performed to amplify the target sequence. Primer and probe sequences for real-time PCR were as follows: Realtime SEOS F (5′-TATGGTTGC-CTGGGGAAAG-3′), Realtime SEOS R (5′-GCT-CTGGATCCATGTCATCA-3′) and probe no. 86 (5′-GCAGTGGA-3′). Hantavirus sequences were then amplified by PCR using primers for the S and M segments as follows: MurS110F (5′-CAGAAGG-TIAIGGATGCAGA-3′), SEOS1589R (5′-ACTTA-AGGTGACCTGGCCCT-3′), SEOM1277F (5′-TT-TAGAGCAGCTGAGCAGCAGAT-3′) and M12–3161R (5′-AACCACTATGGCCACCTTTC-3′).

PCR products were purified and DNA sequencing was performed as described previously [5]. Phylogenetic relationships among the hantavirus sequences were evaluated using the Neighbour-Joining (NJ) program with the Kimura two-parameter distance in CLUSTALW version 1.83 (European Bioinformatics Institute, UK). The phylogenetic tree was visualized using the NJ plot program. Bootstrap resampling analysis was performed using 1000 replicates.

The viral sequence data obtained in this study were deposited in DDBJ/EMBL/GenBank (accession numbers: AB674759–AB674769).

Statistical analysis

Differences between seroprevalence and body weight were examined for statistical significance by the Mann–Whitney U test. P values $<0{\cdot}05$ and $<0{\cdot}01$ were considered significant. Differences in seroprevalence, sex and geographical origin were examined for statistical significance by Pearson's χ^2 test or Fisher's exact test. To estimate the relationship of co-infection of a human pathogen in the rodents, we obtained an estimate from each study of the odds ratio (OR) with 95% confidence interval (95% CI).

RESULTS

Prevalence of antibodies to rodent-borne pathogens

The trapping rates of rodents in Hanoi City and Hai Phong Port were 32·0% and 15·0%, respectively. Prevalence of antibodies against four rodent-borne pathogens is given in Table 1. Antibodies against *L. interogans* were detected in 21·7% (13/60) and 26·5% (9/34) of *R. norvegicus* captured at Hanoi City